nature reviews cardiology

https://doi.org/10.1038/s41569-022-00805-7

Review article

Check for updates

Single-cell transcriptomics for the assessment of cardiac disease

Antonio M. A. Miranda[1] ✉, Vaibhao Janbandhu[2,3], Henrike Maatz[4], Kazumasa Kanemaru[5], James Cranley[5], Sarah A. Teichmann[5,6], Norbert Hübner[4,7,8], Michael D. Schneider[1], Richard P. Harvey[2,3,9] & Michela Noseda[1] ✉

Abstract

Cardiovascular disease is the leading cause of death globally. An advanced understanding of cardiovascular disease mechanisms is required to improve therapeutic strategies and patient risk stratification. State-of-the-art, large-scale, single-cell and single-nucleus transcriptomics facilitate the exploration of the cardiac cellular landscape at an unprecedented level, beyond its descriptive features, and can further our understanding of the mechanisms of disease and guide functional studies. In this Review, we provide an overview of the technical challenges in the experimental design of single-cell and single-nucleus transcriptomics studies, as well as a discussion of the type of inferences that can be made from the data derived from these studies. Furthermore, we describe novel findings derived from transcriptomics studies for each major cardiac cell type in both health and disease, and from development to adulthood. This Review also provides a guide to interpreting the exhaustive list of newly identified cardiac cell types and states, and highlights the consensus and discordances in annotation, indicating an urgent need for standardization. We describe advanced applications such as integration of single-cell data with spatial transcriptomics to map genes and cells on tissue and define cellular microenvironments that regulate homeostasis and disease progression. Finally, we discuss current and future translational and clinical implications of novel transcriptomics approaches, and provide an outlook of how these technologies will change the way we diagnose and treat heart disease.

Sections

[1]National Heart and Lung Institute, Imperial College London, London, UK. [2]Victor Chang Cardiac Research Institute, Sydney, NSW, Australia. [3]School of Clinical Medicine, Faculty of Medicine, UNSW Sydney, Sydney, NSW, Australia. [4]Max Delbrück Center for Molecular Medicine in the Helmholtz Association, Berlin, Germany. [5]Cellular Genetics Programme, Wellcome Sanger Institute, Wellcome Genome Campus, Hinxton, UK. [6]Deptartment of Physics, Cavendish Laboratory, University of Cambridge, Cambridge, UK. [7]Charite-Universitätsmedizin Berlin, Berlin, Germany. [8]German Center for Cardiovascular Research (DZHK), Partner Site Berlin, Berlin, Germany. [9]School of Biotechnology and Biomolecular Sciences, UNSW Sydney, Sydney, NSW, Australia.
✉e-mail: a.almeida-miranda@imperial.ac.uk; m.noseda@imperial.ac.uk

Key points

- A good experimental design requires a matching of the protocol workflow to the cells of interest and scientific goals.
- The generation of reference heart cell atlases and standardized annotations is necessary for cross-study comparisons and accurate data interpretation.
- Emerging disease gene signatures reveal cell-state-specific changes, which will facilitate the generation of novel putative biomarkers and therapeutic targets.
- The definition of cellular microenvironments requires deconvolution with spatial and multi-omics approaches.
- The density of information from these novel omics approaches will contribute to the design of computational models to predict disease, stratify patients and facilitate drug discovery.

Introduction

The human heart is a dynamic organ composed of four morphologically and functionally distinct chambers, as well as highly specialized subdomains including the conduction system and valvular apparatus, all working in synchrony due to the perfectly coordinated actions of billions of cells. In each chamber and anatomical subdomain, diverse stimuli converge on the local cells, priming gene expression patterns that drive phenotypic and functional adaptations, cumulatively determining organ function. Indeed, this fine cellular orchestration facilitates not only continuous contraction and relaxation of cardiomyocytes, but also the effective responses to haemodynamic changes during prenatal and postnatal development, and adulthood.

During embryonic development, the cellular progenies of first and second heart fields are primed in utero, and exposure to haemodynamic changes contributes to their gene expression programmes and maturation after birth[1,2]. In disease states, perturbations to the normal cellular repertoire and microenvironments caused by noxious stimuli, such as mechanical, electrical, chemical or ischaemic damage, can disrupt the transcriptional landscape[3–6]. Gene expression is not merely an epiphenomenon, but rather an essential step in the implementation and amplification of pathogenetic circuits[3,7]. Therefore, studying cellular transcriptional signatures is essential for gaining a robust understanding of organ and tissue function.

Cardiovascular disease remains the leading cause of death globally[8]. Ischaemic heart disease, more specifically, is the foremost cause of death in both men and women, despite robust efforts in the field of preventative cardiology. Furthermore, heart failure (HF), a cardiac functional impairment secondary to many aetiologies, is a rising global epidemic and, despite a growing number of treatments[9–11], transplantation remains the only definitive cure. Therefore, an urgent need exists for novel effective and targeted therapies with more precise risk stratification, which necessitates a deeper understanding of the underlying molecular mechanisms driving the progression of cardiac disease.

Single-cell omics technologies, and especially transcriptomics, have revolutionized the way we investigate organs and organisms, allowing an unprecedented level of resolution in the assessment of cell demographics during both health and disease[12]. Single-cell transcriptomics provides information on gene expression prevalence and heterogeneity as well as co-expression of genes at the individual cell level to facilitate a cell-centric outlook. This approach involves the definition of novel cell markers and transcriptional signatures to delineate cell types (well-established cellular lineages) and cell states (encompassing subtypes or transient, functional cellular transcriptomics signatures) with high accuracy, either manually or using automated computational pipelines[13–15]. Analysis of gene sets enriched in cell types or states allows functional inferences on intracellular regulatory networks and on intercellular pathways across specific cells by focusing on genes encoding ligand–receptor pairs[16,17]. Such analyses highlight the processes underlying coordinated cellular communication that are otherwise masked in bulk analysis.

In this Review, we discuss the latest findings obtained using single-cell transcriptomics that advance our understanding of cardiac biology, development and disease. We explain how we can maximize the implementation of these technologies to study cardiac disease and provide an outlook on multimodal integration with spatial transcriptomics and epigenetics.

Successes and challenges in experimental design

The implementation of single-cell transcriptomics consists of several steps, from tissue processing for cell isolation to single-cell capture, reverse transcription, complementary DNA amplification and library construction, which are followed by sequencing and computational analysis[12,18,19]. In this section, we describe the most successful experimental designs utilized to profile cardiac cells, discuss their advantages and disadvantages, and highlight the need for careful experimental planning and validation options.

Cell types of interest dictate protocol choice

Most single-cell capturing methods including flow cytometry, microfluidics and microdroplet-based systems have an upper size limit for cells of ~25–40 μm[20,21]. Therefore, if the study focuses on cardiac stromal, vascular and immune cell compartments with no major size limitations, these capturing techniques can be used to select single cells for RNA sequencing[22–26] (Fig. 1). However, in the mammalian adult heart, cardiomyocytes pose a major challenge because they are large, rod-shaped cells of approximatively 20 μm in width and 100 μm in length[27]. Micromanipulation or laser capture of cardiomyocytes is possible, but these approaches are limited by low throughput and are operator-dependent[7]. Flow cytometry sorting of cardiomyocytes has been reported, although the length of sorted cardiomyocytes was ~50 μm, suggesting a bias for smaller cells or contracted cells during processing[28,29]. The sorting of cardiomyocytes with preserved RNA quality and function has been achieved using a specialized fluorescence-activated cell sorting (FACS) instrument with a large 500 μm nozzle. However, this type of instrument is not routinely available. Furthermore, the complexity and length of the cardiomyocyte isolation process can potentially affect the resulting transcriptional signature[30]. Single-cell RNA sequencing (scRNA-seq) technologies are limited not only by inefficiency in capturing adult cardiomyocytes, but also by the fact that adipocytes cannot be captured using single-cell isolation protocols. Moreover, an under-representation of cells such as pericytes and fibroblasts is also common in scRNA-seq[27,31]. Therefore, if the aim of the study is to assess and capture all cardiac cell types, profiling single nuclei by using single-nucleus RNA sequencing (snRNA-seq) is the most effective method[27,32–37]. Importantly, snRNA-seq generates largely overlapping molecular signatures with scRNA-seq in the adult human heart[27] and

during cardiomyocyte differentiation in vitro[38]. Furthermore, unlike snRNA-seq, single-cell isolation for scRNAseq requires fresh tissue, and enzymatic and mechanical methods used for single-cell dissociation can risk inducing stress-related transcriptional artefacts, especially when performed at 37 °C for >1 h[39]. The testing of RNA quality from a fresh or frozen tissue sample is recommended. Of note, there are also some caveats in the use of snRNA-seq. snRNA-seq is not ideal for cells such as neurons, in which crucial mRNA trafficking along the axon to the synapse would be missed[40]. Likewise, with snRNA-seq, data from binucleated or multinucleated cardiomyocyte nuclei and data from single-nucleated cardiomyocyte nuclei cannot be distinguished. Additionally, under-representation of endothelial cells in snRNA-seq studies has been reported, which varies according to the protocol used[27,31]. Taken together, snRNA-seq is an effective tool for obtaining comprehensive data from cardiac tissue, and its integration with scRNA-seq maximizes the coverage of cell types and states[27].

Purification and enrichment

The assessment of large numbers of cells that are present at low frequency, such as immune cells, requires antibody-based approaches for enrichment by flow cytometry or immunomagnetic beads. In animal models, specific cell lineages or rare cells, including epicardial cells, can be enriched using methods involving cell tracers such as genetic fate mapping, which involves insertion of a heritable gene encoding a fluorescent protein[41–43]. After isolation, the nuclei are purified to remove the cytoplasmic debris resulting from deliberate disruption of the cytoplasm to release the nucleus. This filtering step can be performed by FACS[27,37,44–46], differential centrifugation or straining[33,47], or by density gradient separation[48] (Fig. 1). The effectiveness of differential centrifugation depends on pipetting skills, and the use of filters with a pore size as small as 10 µm can introduce bias[47]. Indeed, the nuclei of mammalian cells have an estimated size of 8–12 µm[37], or even larger under certain conditions such as in hypertrophic cardiomyocytes[49]. The use of a strainer alone can let through small tissue fragments and debris that can increase background noise[33]. Density gradient centrifugation is also highly operator-dependent and is unsuitable for small volumes with few nuclei[50]. Although FACS purification requires specialized instruments and expertise, this approach ensures good purification of nuclei given that the nozzles are typically ≥70 µm[32,33,47]. Visual inspection of nuclei to confirm nuclear membrane integrity and absence of blebbing and tissue debris is recommended after purification[37]. Of note, a FACS protocol based on immunolabelling of the cardiomyocyte-specific protein pericentriolar material 1 and Hoechst staining for DNA content allow the isolation and profiling of diploid

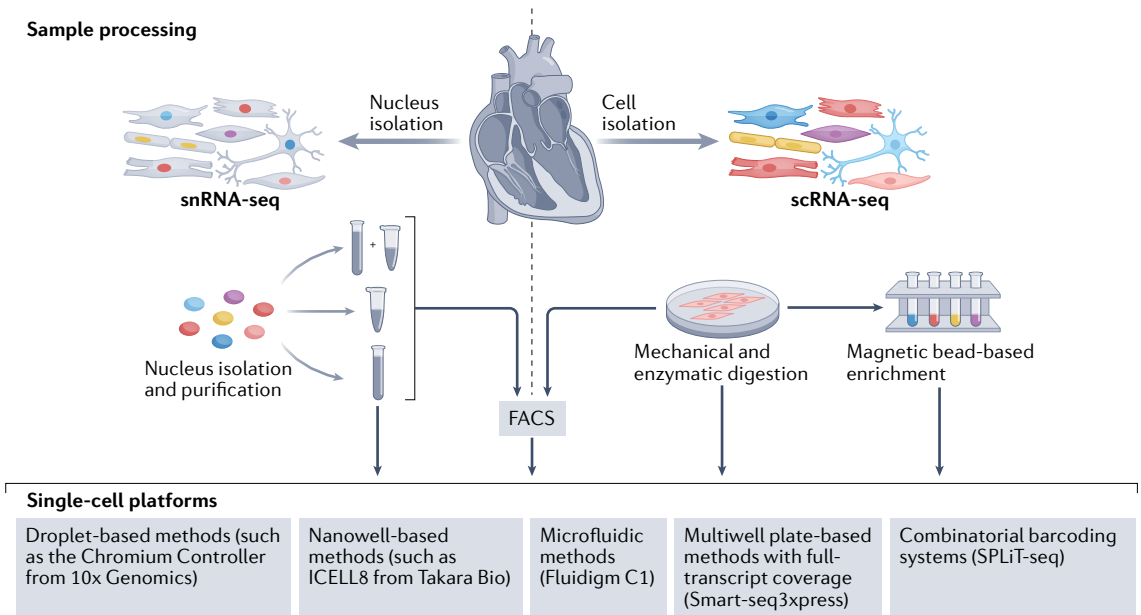

Fig. 1 | Workflow for single-cell and single-nucleus transcriptomics. The design and execution of single-cell experiments involves a multistep process that requires careful planning. The assessment of cardiomyocytes is challenging given that they are too large to be selected as single cells using fluorescence-activated cell sorting (FACS) or most microfluidics-based methods. If all cardiac cell types need to be analysed, the isolation of single nuclei from frozen samples is currently the most commonly used approach, given that this technique allows capture of all known cardiac cell types at the highest throughput. Nucleus isolation requires enzymatic and mechanical dissociation, often with the use of a Dounce homogenizer to help release the nuclei. Before proceeding to library preparation, nuclei can be purified by filtering and then by FACS, or less-stringent protocols include differential centrifugation before filtering and alternatively density gradient centrifugation. If only non-cardiomyocyte cells are needed, mechanical and enzymatic tissue dissociation of fresh samples allows the recovery of stromal and interstitial cells. For rare cell types of interest, the potential enrichment for specific populations can be achieved via antibody labelling of cell surface markers, followed by magnetic bead-based enrichment or flow cytometry sorting. These enriching methods can also be used to select cells expressing fluorescent proteins, such as in lineage-tracing experiments. After the isolation and purification steps, single cells and nuclei are captured, labelled (by barcoding) and incorporated into a library preparation using a variety of single-cell platforms: droplet-based approaches, such as the Chromium Controller from 10× Genomics, which have a high throughput; nanowell-based methods, such as: the ICELL8 instrument from Takara Bio, which allows the selection of a wide range of cell sizes with low-to-medium throughput; microfluidics approaches, such as the Fluidigm C1 platform; multiwell plate-based protocols, such as Smart-seq3xpress; and methods based on multiple rounds of splitting and pooling of cells, such as SPLiT-seq, which allow the barcoding of single cells without the need for physical separation. scRNA-seq, single-cell RNA sequencing; snRNA-seq, single-nucleus RNA sequencing.

versus tetraploid nuclei, a key step in defining the transcriptional changes occurring in neonatal proliferating cardiomyocytes[48,51]. However, certain dyes used for nuclei sorting can intercalate between DNA base pairs and disrupt chromatin structure[52]. Therefore, when downstream analysis includes single-nucleus assay for transposase-accessible chromatin sequencing (snATAC-seq), a recommended dye such as 7-aminoactinomycin D should be used. In addition, during FACS, nuclei shear stress, high hydrodynamic pressure and osmotic changes could induce chromatin rearrangement[53]. By contrast, these effects are unlikely to influence gene expression when the nuclei are isolated from frozen tissue and experiments are performed at 4 °C, which prevents the activation of transcription[27,37,44–46].

Available single-cell or single-nucleus platforms

After choosing the best protocol for cell and nucleus isolation, the next crucial decision is the optimal method for single-cell and single-nucleus capture and library construction[20,54,55] (Fig. 1). Microfluidic systems (such as the Fluidigm C1 platform) were among the first systems used to study heart cells; however, a low-to-medium throughput and high costs have limited their use[20,23]. In droplet-based platforms (such as 10× Genomics and Drop-seq technologies), thousands of isolated single cells or nuclei are moved through advanced microfluidic devices, where they are individually partitioned with uniquely barcoded beads into nanolitre-sized gel emulsions[56,57]. These platforms allow the capture of typically 5,000–10,000 cells or nuclei per sample with low costs, enabling a wide representation of cell populations, including rare cell types. Technologies based on full-length transcriptome sequencing, such as Smart-seq3, allow the characterization of transcript isoforms facilitating the detection of a larger number of transcripts per cell than droplet-based approaches, but at higher costs per cell and with lower throughput[58]. However, protocol updates in the past year (Smart-seq3xpress) have substantially increased the throughput while maintaining high sensitivity[59]. Nanowell-based technologies include ICELL8 (Takara), a mid-throughput platform that combines imaging and dispensing of single cells into nanowells to capture hundreds of cells with a wide range of sizes, including cardiomyocytes[60–62]. Finally, SPLiT-seq is an alternative affordable method based on combinatorial barcoding that does not require single-cell capture, is compatible with fixed cells and nuclei, and can be used for large cardiomyocytes[63].

Capturing anatomical diversity

Designing cardiac single-cell or single-nucleus transcriptomics experiments requires careful consideration of the multiple (sub)anatomical regions of the heart, which consists of highly specialized structures with a diverse cellular composition. The most comprehensive human heart reference cell atlas involved the collection and analysis of six anatomical regions: the right ventricle (RV) and left ventricle (LV) free wall, apex, interventricular septum, and right and left atria[27]. According to snRNA-seq data, the atria and ventricles of donor hearts have different cellular compositions, with an inverse correlation between the proportion of fibroblasts and cardiomyocytes, in accordance with the role of the ventricles as the primary pumping chambers[27]. Analysis of the aortic valve and aorta was challenging, owing to the paucicellular nature of the tissue and its richness in extracellular matrix (ECM)[64,65]. Although some studies have explored anatomical differences during mouse development to define progenitor cells beyond the known first and second heart fields[23,41,42,66], an unmet need exists for a systematic analysis of chamber differences in the adult mouse heart. Indeed, analyses with higher precision and broader spectrum of anatomical regions are needed for consistent comparisons across studies, species and disease phenotypes.

Power calculations

Two additional aspects are crucial in the design of scRNA-seq and snRNA-seq experiments: the number of single cells or nuclei to be analysed per sample and the depth of sequencing, which influences the number of genes obtained per cell. Most experiments are designed to obtain data from thousands of single cells with relatively shallow sequencing, or from hundreds of cells with deeper sequencing. The choice of approach can be qualitatively assessed in exploratory studies or on the basis of emerging tools for power calculations. The web-based single-cell one-sided probability interactive tool (SCOPIT) estimates the necessary number of cells to be sequenced to resolve cell types present at different frequencies[67], whereas the statistical framework scPower models the relationship between the number of cells per individual, sequencing depth, sample size and power of differentially expressed genes within cell types to compare a multitude of experimental designs and to optimize the design within a limited budget[68]. In general, the sequencing of a large number of cells at a lower depth leads to higher power compared with sequencing fewer cells at a higher depth[68]. Nevertheless, deeper sequencing of hundreds of cells can be useful to characterize prospectively sorted rare populations. Regarding biological replicates, proof-of-feasibility experiments have largely been conducted with a low number of replicates[22,26], but now the field has reached a phase in which variability can be predicted for both animal and human studies. In human cardiomyopathies involving pathogenic variants affecting the same gene, a cohort of five individuals has been shown to be sufficient to highlight statistically significant differences in gene expression and other related parameters, including cellular composition[69].

The importance of metadata

For best practice, to reduce the risk of technical bias, studies should, if possible, incorporate cells or nuclei obtained with the same protocol, especially when performing comparisons across different treatment groups or diseases and controls. Indeed, the various protocols for the isolation and purification of cells and nuclei can have different effects on the proportions of the types and states of cells retrieved, as well as on their transcriptional and epigenetic signatures. Moreover, substantial structural changes in pathological tissue or analysis of different anatomical regions of the heart, such as highly fibrotic tissue, could affect the release of certain cell types, even when using the same protocol. Therefore, reporting technical metadata and histopathological evaluation of the tissue microstructure for each sample is important to facilitate accurate data interpretation and integration across studies. Consequently, cell annotation and compositional analysis need to be evaluated in the context of the experimental design, and require validation with multiple platforms, including high-resolution spatial transcriptomics.

Overview of the computational workflow

Computational analysis of scRNA-seq or snRNA-seq data is a complex multistep process that requires specialized expertise (Fig. 2). In this section, we provide an overview of the crucial steps[70].

Quality control and data integration

Analysis pipelines for processing raw data, such as Cell Ranger[57], SEQC[71] and zUMIs[72], perform initial quality checks[73] on the sequencing reads, demultiplex data by assigning reads to their cellular barcodes and

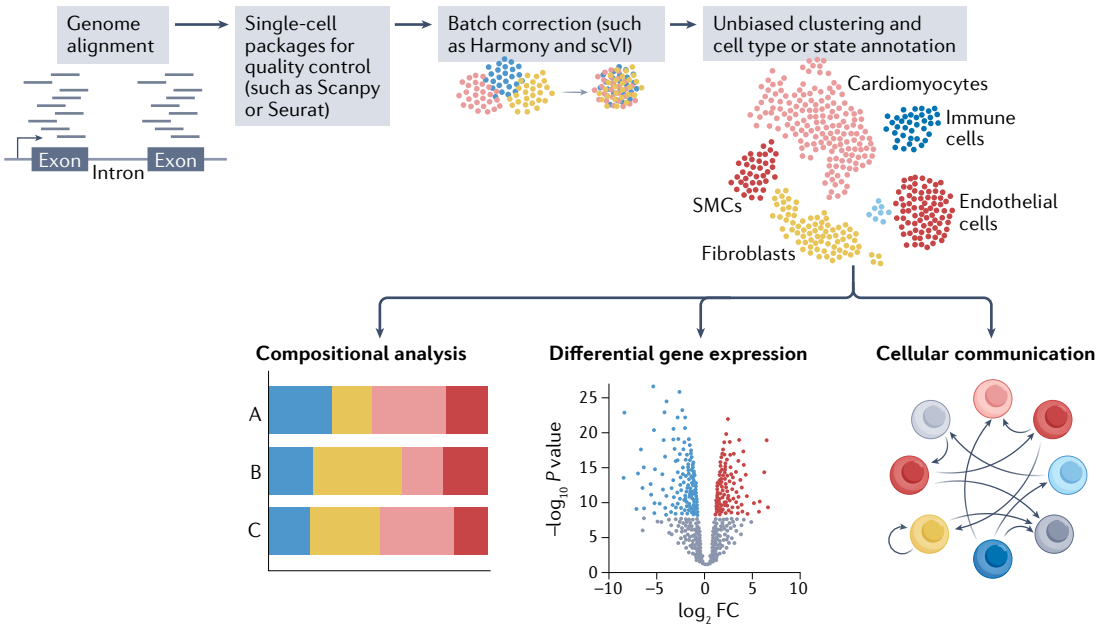

Fig. 2 | Computational analysis workflow. After the sequencing of libraries, the overall bioinformatics pipeline is largely the same, regardless of which sampling procedure was chosen. After aligning the reads to a reference genome, comprehensive single-cell packages (such as Scanpy and Seurat) are used for quality control, batch correction and data integration. A key step in this process is the clustering and annotation of cell types and states, which is performed on the basis of the expression of known marker genes and the interpretation of the transcriptional signatures of each cluster. Of note, deep learning-based approaches are emerging for automated annotation. Comprehensive annotation facilitates increased resolution in complex downstream analyses, such as: compositional analysis (the proportion of various cell types present in a tissue across various conditions); differential expression analysis between different diseases or treatments; and inferences on intercellular communication on the basis of the expression of genes encoding ligand receptors in different cell types and states. FC, fold change; SMCs, smooth muscle cells.

mRNA molecules of origin, and facilitate genome alignment and quantification. In droplet-based scRNA-seq and snRNA-seq analyses, the degree of contaminating ambient transcripts released into the cell or nucleus suspension during tissue dissociation can vary according to the dominant cell types and might lead to misinterpretation of the results. In the human heart, cardiomyocyte nuclei are the major contributors to ambient contamination. Software tools, such as CellBender, SoupX and DecontX, can minimize technical artefacts in data[74–76]. For example, CellBender can estimate ambient RNA from empty droplets and correct the expression metrics by removing counts related to ambient RNA molecules and even random barcode swapping[74–76].

Standard quality control includes establishing minimum and maximum numbers of reads and genes per cell or nucleus, and determining a threshold for the highest percentage of genes encoding ribosomal proteins and mitochondria per cell or nucleus, above which a cell is defined as poor quality or unhealthy[73]. Single-cell analysis of cardiomyocytes needs to take into consideration the high proportion of mitochondria normally present in cardiomyocytes compared with other cells[77]. Two or more cells or nuclei that are attached, captured within the same droplet or microwell, and represented by the same barcode can generate a hybrid transcriptome, an artefact that violates the fundamental principle of single-cell technology and results in incorrect inferences. Doublet or multiplet detection is best performed using unbiased methods such as Scrublet and SOLO, which involve simulation of doublets or multiplets to create a training set for a machine learning classifier[70,78,79]. Correct and precise identification of doublets is necessary to avoid the risk of confusing artefactual chimeric hybrids derived from two (or more) cells adhered together with transitional cell states.

To overcome batch effects and unwanted technical variation while retaining biological differences, multiple integration methods can be applied[80,81]. The assembly of one of the largest human donor heart cell atlases involved the successful integration of data from single nuclei and cells from 14 donor hearts, in which differences between ventricles and atria were retained, as well as left and right specificities[27]. Successful data integration was also observed in two studies of human hearts from individuals with HF that included analyses of >800,000 nuclei[47,69].

Defining cell types and states

The annotation of cell types and states is a complex task that is necessary for data interpretation. The major cardiovascular cell types include cardiomyocytes, fibroblasts, endothelial cells, smooth muscle cells (SMCs), pericytes, immune cells, neuronal and glial cells, and adipocytes. Most of these cell types have multiple identifiable cell states with anatomical specificities[22–24,27,33,82]. Cell annotation requires unbiased clustering and the analysis of the expression of known marker genes and novel gene signatures. Unbiased clustering is a key step, the results of which depend on algorithm resolution and the number of droplets analysed: a high resolution will determine a high number of cell states or types, whereas lower granularity will be obtained with lower resolution. Each study will apply a given resolution with a subjective final decision that influences the results, which together with the effectiveness of data integration, doublet exclusion and ambient contamination subtraction

can affect the accuracy of comparisons across studies. Computational tools that can be used to estimate the best resolution include SCCAF[83] and MultiK[84]. However, it is imperative to assess whether differentially expressed genes across the various clusters are clearly defined and are biologically meaningful. The annotation of the identified cell clusters (each of which represents a cell type or state) is mostly performed manually on the basis of transcriptional signatures. However, owing to the availability of open reference data, label transfer approaches are possible for some tissue systems such as immune cells. CellTypist and scNym can automatically annotate cell types or states in a query dataset by mapping them onto a reference[13,85]. The creation of databases and collaborative initiatives will be needed to form a consensus on the optimal approach to the annotation of cardiac cell types and states for accurate comparisons across studies. Furthermore, the use of novel deep learning strategies such as scArches, which is based on transfer learning, enables efficient building and sharing of reference atlasing data and to retain disease variation when mapping to a health reference, as shown for coronavirus disease 2019 (COVID-19) datasets[86]. Such approaches will be key to ensuring the efficient use of the human cardiac reference atlas to improve our understanding of disease and to create model organism atlases that will facilitate functional validations.

Integration of multimodal omics approaches

The integration of data across multiple modalities such as scRNA-seq and snRNA-seq, ATAC-seq or proteomics can generate standardized cell state labels[87–89]. Computational tools such as cell2location and Giotto allow mapping of newly defined cell types and states onto the physical 2D space by combined analysis of scRNA-seq or snRNA-seq data with spatial transcriptomics (analysis of gene expression on tissue sections)[27,90–92]. This integration is needed because of the intrinsic nature of current spatial transcriptomics technologies that are based on the analysis of microtiles of tissue typically encompassing 5–15 cells, although this number varies depending on the size of the tile and the size of the cells captured, resulting in microbulk gene expression data. Integration tools allow the deconvolution of this microbulk information and the mapping of specific cells in space, which guides the definition of cellular niches. One typical spatial transcriptomics method, such as the commercially available Visium by 10x Genomics, is based on positioning tissue samples on slides covered with unique barcoded mRNA-binding oligonucleotides, which facilitates the capture of RNA from the tissue with high spatial resolution (protocols are available for frozen sections and formalin-fixed paraffin-embedded (FFPE) sections)[93,94]. Alternatively, individual RNA molecules can be directly profiled using the Nanostring GeoMx Digital Spatial Profiler, which assigns fluorescently labelled barcoded probes to genes of interest that are hybridized on the tissue and subsequently counted by a computerized optical lens without the need for amplification (compatible with FFPE sections)[95]. Non-commercially available protocols such as Slide-seq have also been developed, which involve the use of barcodes to capture RNA with a resolution of 10 μm[94].

Together, the assembly of large atlases from publicly available datasets representing tens to hundreds of individuals will contribute to the definition of consensus cardiac cellular maps by characterizing common signatures across multiple studies[96]. Larger multi-organ studies such as the Tabula Sapiens[97] overcame difficulties of integrating data from diverse organs, including the heart, paving the way to a new series of studies focusing on the definition of shared and organ-specific molecular signatures of cells present across the whole body, such as fibroblasts, vascular cells and immune cells[98]. This step is crucial for the definition of putative organ-specific and tissue-specific cellular therapeutic targets. Likewise, the computational analysis of scRNA-seq and snRNA-seq data and its integration with other modalities is a fundamental and demanding step that requires interdisciplinary expertise for accurate hypothesis generation and functional inferences.

Cardiomyocyte profiling in health and disease

Isolating large numbers of rod-shaped cardiomyocytes from cardiac tissue is inherently difficult and requires manual micropipetting or dispenser approaches using a large nozzle size. Consequently, only a few studies have characterized gene expression by scRNA-seq in single, freshly isolated adult human cardiomyocytes[7,61].

Cardiomyocytes in the healthy heart

snRNA-seq has emerged as a successful high-throughput transcriptomics approach for profiling adult human cardiomyocytes[27,32,33] and has revealed previously unknown inter-compartmental and intra-compartmental cardiomyocyte heterogeneity between cardiac regions of donor hearts[27,33] (Table 1). Although the transcriptional diversity between atrial and ventricular cardiomyocytes probably reflects different developmental origins and electromechanical stimulations, distinct genomic signatures of cardiomyocyte subpopulations within anatomical regions suggest additional functional diversity that might correspond to specific tissue microenvironments. Such subpopulations include cardiomyocytes enriched for retinoic acid-responsive genes and stress-response-related genes, as well as cardiomyocytes enriched for nuclear-encoded mitochondrial genes indicative of a high energetic state, which suggests that these cardiomyocytes are equipped for a higher workload[27]. Interestingly, these cardiomyocyte states have been found in both atrial and ventricular cardiomyocytes[27]. However, whether their localization is enriched in areas of increased wall stress within the ventricle or atrium and how they vary under different pathological conditions, such as mitral or tricuspid valve disease, remains unknown. Likewise, the differences between the transcriptional signatures specific to the cardiomyocytes of the spirally oriented ventricular muscle fibres that constrict the chamber and those of the trabecular cardiomyocytes remain unclear[99]. A novel cardiomyocyte state enriched for *Myoz2*, which encodes the calcineurin inhibitor myozenin 2, was localized just below the epicardial surface of the mouse heart[28], supporting the hypothesis that specific cardiomyocyte states localize to defined microenvironments.

Prenatal cardiomyocyte development

Analysis of human fetal hearts at 5–25 weeks of gestation has led to the identification of cell clusters composed of trabecular, ventricular and atrial compact myocardium[100]. Key transcription factors, such as *HAND2* and *NR2F1* (encoding heart and neural crest derivative-expressed protein 2 and COUP transcription factor 1, respectively), were identified in atrial cardiomyocytes, whereas *HAND1* and *HEY2* (encoding hairy/enhancer-of-split related with YRPW motif protein 2) were found in ventricular muscle cells. At 5 weeks, proliferating cardiomyocytes were observed, as well as muscle cells with key left-side specification genes (*IRX3*, encoding iroquois-class homeodomain protein IRX 3 in ventricular compartments, and *PITX2* encoding pituitary homeobox 2 in atrial compartments)[100]. At 19–22 weeks, a population of proliferating cardiomyocytes showed high expression of *TOP2A* (encoding DNA topoisomerase 2α) and *MKI67* (encoding proliferation marker protein Ki-67), as well as a lack of expression of *TCAP* (encoding telethonin, a protein needed for the assembly of mature myofibrils)[101]. An understanding

Table 1 | Cardiomyocyte gene signatures identified with omics technology

Setting	Mouse	Human
Health	Neonatal: *Cited1* and proliferative markers such as *Nrg1*, *Erbb2*, *Nfya* and *Nfe2l1* Adult: *Myoz2*$^{+}$ (subepicardial)	Neonatal: *CITED2*, *CITED4*, *HAND2*, *NR2F1*, *PITX2* and *RELN* (localized to the atria); *HAND1*, *HEY2*, *IRX3*, and ECM-related genes (localized to the ventricles) Adult: stress-response-related genes and nuclear-encoded mitochondrial genes (in cardiomyocytes)
Ischaemic injury	*B2m* (myocardial infarction model)	↑ Expression of genes related to targeting of proteins to the endoplasmic reticulum and energy metabolism ↑ Expression of genes localized at the injury zone (*ANKRD1*$^{+}$*NPPB*$^{+}$) and the middle of the border zone (*ANKRD1*$^{+}$*NPPB*$^{-}$)
HCM	↑ Expression of *Nppa*, *Nppb* and genes related to glycolysis and p53 signalling ↓ Expression of calcium handling-related genes, metabolism-related genes and *Ephb1* (TAC model)	↓ Expression of *EPHB1*, *ERBB4* and *FGF12*
DCM	Not reported	Gene programmes related to contractility and glycolysis Genotype-specific changes: ↑ expression of *SH3RF2* (in patients with no pathogenic variants) and ↑ expression of *FNIP2* (in patients with variants in *LMNA*)
CHD	Not reported	Gene programmes related to EGFR signalling and FOXO signalling ↑ *CRIM1* to *CORIN* ratio

CHD, congenital heart disease; DCM, dilated cardiomyopathy; ECM, extracellular matrix; EGFR, epidermal growth factor receptor; FOXO, forkhead box protein O; HCM, hypertrophic cardiomyopathy; TAC, transverse aortic constriction.

of the gene expression signatures present in proliferating cells is key to identifying cardiomyocytes with a predisposition to divide and to define potential therapeutic strategies for heart regeneration. In this regard, a comparison of gene expression signatures across different time points in prenatal and postnatal periods is needed.

Of note, a comparison of the cardiac cellular landscape in human versus that in mouse fetal hearts suggested differences in gene expression signatures between the two species[23,100,102,103]. Although cardiomyocytes were the most similar among all cell types, ventricular cardiomyocytes in humans expressed ECM-encoding genes earlier and more abundantly than those in mice. *RELN* (encoding reelin) expression was specific to human atrial trabecular cardiomyocytes and was absent in mice[23,100,102,103]. Furthermore, *CITED2* (encoding Cbp/p300-interacting transactivator 2) and *CITED4* were enriched in developing human cardiomyocytes, whereas *Cited1* was enriched in the mouse counterpart[23,100,102,103] (Fig. 3).

Cardiomyocytes in disease

Myocardial infarction. In a mouse model of myocardial infarction (MI), scRNA-seq identified a cardiomyocyte subset with upregulated expression of β2 microglobulin in response to ischaemic damage[29]. In vitro experiments suggested that this upregulation drives fibroblast activation. Furthermore, a multimodal approach combining snRNA-seq, snATAC-seq and spatial transcriptomics was used to study cardiac samples from hearts explanted 2–5 days after the onset of clinical symptoms of MI, before the patients received a total artificial heart[104]. This integrated method allowed the investigators to map putative enhancers controlling gene expression within distinct cardiomyocyte niches of injury, repair and remodelling, revealing a regional influx of immune cells in response to localized induction of cytokines, and defined *RUNX1* (encoding runt-related transcription factor 1) as a potential driver of myofibroblast differentiation[104]. The inclusion of spatial transcriptomics helped to determine localized differences at the site of ischaemic injury. *ANKRD1* (encoding the transcriptional repressor ankyrin repeat domain 1, the overexpression of which has been shown to impair cardiomyocyte function[105]) and *NPPB* (encoding natriuretic peptide B, which is widely used as a marker for cardiac disease and is upregulated in the border zone after MI in mice[106,107]) were defined as markers for two niches of stressed cardiomyocytes[104]. Importantly, integration with snATAC-seq facilitated the identification of T-box protein 3 (TBX3) and myocyte-specific enhancer factor 2D as regulators of an *ANKRD1*$^{+}$*NPPB*$^{-}$ pre-stressed cell state, and cyclic AMP-dependent transcription factor ATF3 as a driver of the *ANKRD1*$^{+}$*NPPB*$^{+}$ state[104].

Cardiac hypertrophy. A multimodal approach including epigenetic, morphological and functional assessment and co-expression network analysis of mouse and human single cardiomyocyte transcriptomes has facilitated the delineation of conserved mechanisms of pressure overload responses[7]. In early hypertrophy, cardiomyocytes were found to activate mitochondrial translation and oxidative phosphorylation, which correlated with morphological hypertrophy[7]. Subsequently, sustained overload induced p53 activation, leading to the disruption of adaptive hypertrophy transcriptional programmes and the promotion of HF[7]. This observation confirms that cardiomyocyte identity and morphological and functional phenotypes are encoded in transcriptional programmes.

A snRNA-seq study on pathological cardiac hypertrophy caused by aortic stenosis highlighted the downregulation of ephrins, the largest family of receptor tyrosine kinases, in cardiomyocyte hypertrophy[46]. In particular, a downregulation of *EPHB1* (encoding ephrin type B receptor 1) observed in the human hypertrophic heart was confirmed in a transverse aortic constriction (TAC) mouse model of pressure overload[46]. In vitro treatment of cells with EFNB2, the ligand for EPHB1, rescued the hypertrophic phenotype[46]. A TAC mouse model was used to mimic the progression towards pathological hypertrophy and led to the identification of early metabolic cardiomyocyte adaptation, which was evidenced by an upregulation in the expression of glycolysis-related genes, a continuous increase in the expression of the hypertrophy-related genes *Nppa* and *Nppb*, and a decrease in calcium handling-related genes[108]. In addition, the number of cardiomyocytes enriched for *ERBB4* (encoding receptor tyrosine protein kinase erbB4) and *FGF12* (encoding fibroblast growth factor 12) was reduced in hypertrophied human hearts compared with healthy hearts[46]. To advance our understanding of pathological cardiac hypertrophy, the cardiomyocyte

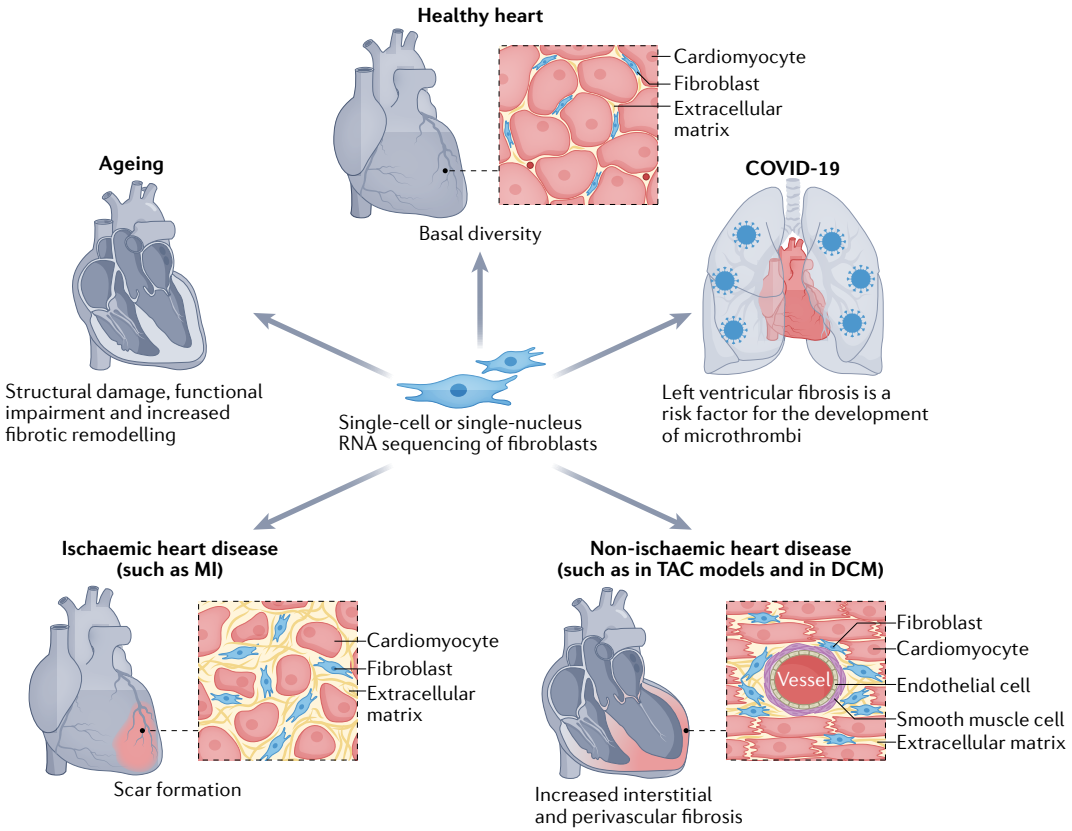

Fig. 3 | Single-cell and single-nucleus analysis revealed previously unknown complexities within fibroblasts. Fibroblasts are key in homeostasis as well as in disease progression, given that fibrosis is a common feature of the response to injury. Single-cell and single-nucleus RNA sequencing have provided insights into the role of fibroblasts in the ageing heart and in different disease settings, such as myocardial infarction (MI) and dilated cardiomyopathy (DCM). A list of fibroblast populations annotated using single-cell and single-nucleus studies is shown in Table 2. COVID-19, coronavirus disease 2019; TAC, transverse aortic constriction.

profile from patients with cardiac hypertrophy of different aetiologies, such as hypertension and hypertrophic cardiomyopathy, should be assessed. Similarly, the specific cardiomyocyte states present in these diseases and their distribution within the tissue remains largely unexplored.

Cardiomyopathy. A convergence of cardiomyocyte transcriptomic changes is thought to be present in the setting of HF associated with dilated cardiomyopathy (DCM)[45]. An analysis of 61 patients with DCM or arrhythmogenic cardiomyopathy (ACM) with defined genetic mutations showed a substantial proportion (20–40%) of differentially expressed genes, suggesting a degree of divergence even in late-stage failing hearts[69]. Specific expression profiles included a general downregulation of *MYH6* (encoding myosin 6) and cell-state-specific upregulation of *SH3RF2* (encoding the anti-apoptotic protein E3 ubiquitin protein ligase SH3RF2) in patients with no known pathological gene variant, and an upregulation of *FNIP2* (encoding folliculin-interacting protein 2, which is involved in the inhibition of oxidative metabolism) in patients with variants in *LMNA* (encoding prelamin A/C) or *PKP2* (encoding plakophilin 2), but not in patients with variants in *TTN* (encoding titin) or *RBM20* (encoding RNA-binding protein 20)[69]. Different HF aetiologies also lead to different cardiomyocyte transcriptomic signatures, suggesting a divergence of pathogenic mechanisms. Cardiomyocytes from failing hearts due to ischaemic cardiomyopathy (ICM) show dysregulation of different gene ontologies from cardiomyocytes from hearts with DCM[62]. For example, ICM causes cardiomyocyte changes in energy metabolism and protein targeting to the endoplasmic reticulum, whereas DCM causes cardiomyocyte changes in muscle contraction[62].

Congenital heart disease. Single-cell transcriptomics has also provided new insights into congenital heart disease. A study of hearts from nine paediatric patients with different aetiologies of congenital heart disease and four control individuals found that age had a minimal contribution to the cardiomyocyte transcriptome compared with disease status[109]. A disease-specific cell state was identified in patients with congenital heart disease, which was characterized by increased EGF receptor (EGFR) and forkhead box protein O signalling, as well as insulin resistance. These transcriptomic changes were validated by scATAC-seq data that showed an increase in chromatin accessibility in 84–90% of differentially expressed genes. The expression of *CORIN* (encoding atrial natriuretic peptide-converting enzyme) was also strongly associated with healthy cardiomyocytes, whereas *CRIM1* (encoding cysteine-rich motor neuron 1 protein) was enriched in diseased cardiomyocytes. This observation was validated by RNA in situ hybridization, which showed that the *CRIM1* to *CORIN* ratio was higher

in cardiomyocytes from patients with congenital heart disease than in those from controls[109].

Cardiac regeneration. The regeneration potential of adult mammalian hearts is very limited and the response after injury is inadequate to reconstitute ventricular cardiomyocyte numbers[110]. However, an analysis of mouse and human failing and non-failing adult hearts revealed subpopulations of cardiomyocytes with cardiac regeneration potential, underpinned by a capacity to dedifferentiate and upregulate cell cycle regulators after stress[34]. In a zebrafish model of heart regeneration after cryoinjury, scRNA-seq defined a subset of cardiomyocytes from the border zone that could partially dedifferentiate, shift their metabolism towards glycolysis and proliferate[111]. Neuregulin 1–ErbB2 signalling contributed to the switch to glycolysis and promotion of cell division in mice and zebrafish[111]. Subsequent snRNA-seq studies of mouse hearts during the early postnatal regenerative window identified immature cardiomyocytes that enter the cell cycle after injury but disappear as the heart loses its regenerative capacity[48]. According to findings from gain-of-function experiments, the unique transcriptional signature of these proliferative cardiomyocytes is related to the activity of nuclear transcription factor Y subunit α and serum response factor[48]. In addition, the endoplasmic reticulum membrane sensors NFE2L1 and NFEL2 drive cardiomyocyte protection[48]. The identification of proliferative cardiomyocytes provides novel inroads for future regenerative therapies.

Fibroblasts in health and disease

Cardiac fibroblasts are dynamic components of the heart's cellular ecosystem that act as lineage progenitors, master conductors of ECM synthesis and remodelling, intercellular signalling hubs and electromechanical transducers[112]. Fibroblasts are also the central component in cardiac fibrosis, which is observed in most forms of cardiac pathology (Fig. 3a). Although initially protective, unresolved fibrosis leads to chamber stiffening and HF, as well as sudden death due to arrhythmias[112]. Many anti-fibrotic drugs have not been successful in improving end points in clinical trials, probably owing to factors such as biological differences between rodent and human hearts, and therapeutic target pleiotropy leading to adverse effects. Therefore, the identification of novel therapeutic targets in cardiac fibrosis is a priority[113–118]. Single-cell genomics have begun to unravel diverse quiescent and activated fibroblast populations in adult hearts[22,24,27,28,119–121] (Table 2).

Human fibroblasts

In the human donor heart cell atlas, in a study with one of the highest number of cells and nuclei assembled to date, five fibroblast populations were identified, including chamber-specific ECM-producing fibroblasts and fibroblasts enriched for cytokine receptor genes such as *OSMR* (encoding oncostatin-M-specific receptor subunit β) and *Il6ST* (encoding IL-6 receptor subunit β), which might modulate immune responses[27]. This cell atlas identified activated fibroblasts that were shown to express pro-fibrotic genes[27]; however, other studies did not show activated fibroblasts in healthy hearts[33,47]. Shifts in the proportion of specific fibroblast populations and their gene signatures in disease states have been observed, including an increase in myofibroblasts enriched for *ELN* (encoding elastin) in patients with DCM[45,122] or ICM[122], as well as an increase in lipogenic fibroblasts enriched for *DLK1* (encoding protein delta homologue 1) in the RV of patients with DCM and in non-ischaemic areas of the LV in patients with ICM[122]. In addition, a decrease in 'resting' fibroblasts (enriched for *PLA2G2A*, encoding membrane-associated phospholipase A2) was observed in patients with DCM[45,122] or ICM[122]. Activated fibroblasts, which are characterized by the expression of *POSTN* (encoding periostin) and *FAP* (encoding fibroblast activation protein), are also consistently increased in HF[45,47,69,122]. However, the extent of the increase in activated fibroblasts might depend on patient genotype, given that the increase was less evident in patients with variants in *LMNA* and *RBM20* compared with patients with *TTN* variants or no known pathogenic variants[69]. In a study of patients with DCM or HCM[47], the best marker of activated fibroblasts was expression of *COL22A1* (encoding collagen α1 (XXII) chain), which was variably detected in patients with DCM or HCM[47]. This finding

Table 2 | Fibroblast populations annotated using single-cell and single-nucleus studies

Fibroblast population	Human		Mouse	
	Healthy	Disease	Healthy	Disease
Quiescent	Annotated	Annotated	Annotated	Annotated
Progenitor-like (*Ly6a*^{high} in mouse)	?	?	Annotated	Annotated
WntX (*Wif1*$^{+}$*Dkk3*$^{+}$)	Not detected	?	Annotated	Annotated
Transitory	Not annotated	?	Annotated	Annotated
Activated (*Postn*$^{+}$)	Annotated	Annotated	Annotated	Annotated
Interferon-responsive	Not detected	?	Annotated	Annotated
Lipogenic (*DLK1*$^{+}$)	Annotated	Annotated	?	?
Responsive to cytokines or chemokines	Annotated	?	?	?
Injury response	Not detected	?	Not detected	Annotated
Pre-proliferative	Not detected	?	Not detected	Annotated
Proliferative	Not detected	Annotated	Not detected	Annotated
Myofibroblasts	Not detected	Annotated	Not detected	Annotated
Matrifibrocytes	Not detected	?	Not detected	Annotated

?, indicates states that need to be further explored.

should be interpreted cautiously, considering that a separate study of patients with DCM or ACM showed genotype-specific upregulation of different collagens, such as *COL4A1* and *COL4A2*, in patients with pathogenic variants in *LMNA*, *TTN* or *PKP2*, and *COL4A5* and *COL24A1* in patients with no known pathogenic variants[69]. Overall, these findings highlight unexpected nuances in the gene signatures of activated fibroblasts, and a need to further understand the relationship between different fibroblast states and their distribution in cardiovascular diseases. A CRISPR-based knockout screen of several genes expressed in cardiomyopathy-associated fibroblast populations uncovered several new regulators of fibrosis, such as *PRELP* and *JAZF1* (encoding prolargin and juxtaposed with another zinc finger protein 1, respectively)[47].

Single-cell and single-nucleus transcriptomics studies of developing, healthy, diseased and partially recovered (unloaded) adult human hearts have confirmed the presence of fibroblast cell state heterogeneity and have highlighted additional regulators of fibroblast differentiation[27,61,100,104,112,123]. Co-localization of myofibroblasts with phagocytic macrophages after MI has also been demonstrated using spatial transcriptomics[104]. Finally, increased expression of *ACE2* (encoding angiotensin-converting enzyme 2) was observed in the fibroblasts of hearts from patients with COVID-19 compared with healthy controls[124], in addition to an enrichment in fibroblasts with prothrombotic, ECM-producing, ECM-organizing and immune cell-related signatures[27,124–129].

Mouse fibroblasts

In mouse ventricles, a predominant quiescent fibroblast subtype ($PDGFRA^{+}SCA1^{high}$ fibroblasts, termed F-SH[24]; also described as progenitor-like state fibroblasts[25]) exists across all organs[130–134], and is enriched in cells with progenitor characteristics such as hypoxic niche and potential for multilineage differentiation, suggesting that these fibroblasts might be a lineage reserve for mobilization after injury[131–133,135,136]. F-Act fibroblasts[24,132], an activated fibroblast population expressing *Meox1* (encoding homeobox protein MOX1 (MEOX1), a transcriptional regulator involved in fibroblast activation during cardiac dysfunction[137]) and *Cilp* (encoding cartilage intermediate layer protein 1), are present at low levels in uninjured hearts, but expand to account for 20–50% of all cardiac fibroblasts by day 3 after MI[24,132], seemingly deriving from more quiescent fibroblasts, or their pre-proliferative and proliferating counterparts[24]. F-Act fibroblasts lack expression of the α-smooth muscle actin gene *Acta2*, and thus might correspond more closely to previously characterized 'proto-myofibroblasts'[112]. Interestingly, *Cilp1*-knockout mice have better cardiac function after MI and a reduced number of myofibroblasts than control mice[138], supporting a key role of *Cilp1* in fibroblast activation and differentiation. F-Act fibroblasts resemble the human $POSTN^{+}FAP^{+}$ fibroblasts mentioned above, but their functional similarity needs validation[112]. Another minor activated fibroblast population in mice, F-WntX[24], expresses genes encoding secreted antagonists of WNT signalling and other pro-fibrotic regulators, one of which, WIF1, is essential for restricting the response of inflammatory monocytes after MI[24,139].

scRNA-seq has enabled investigators to define fibroblast-dependent cytokine pathways that contribute to the inflammatory phase of MI repair[140]. The levels of a fibroblast subpopulation known as injury response cells (IR) peak on day 1 after MI, before decreasing rapidly, and this cell subtype is likely to be involved in the early inflammatory response[25]. IR cells might be similar to pro-inflammatory fibroblasts, previously described in a cardiac pressure overload model, which recruit $Ly6C^{high}$ monocytes via NF-κB signalling and expression of genes encoding monocyte chemoattractants such as CC-motif chemokine 2 (CCL2) and CCL5 (ref.[141]).

The number of myofibroblasts, the most distinctive injury-related fibroblast subtype, peaks at about day 7 after MI in mice[25]. Myofibroblasts can derive from the F-Act pool and/or other activated populations and as they differentiate show downregulation of stem cell markers and massive upregulation of ECM-related and contraction-related genes[25,142]. However, myofibroblast subgroups have different pro-fibrotic or anti-fibrotic regulatory gene signatures, suggesting that fibrosis is self-limiting[24]. Accordingly, myofibroblasts transition to a deactivated, post-proliferative cell type known as matrifibrocytes[143], which are associated with osteogenic and chondrogenic ECM signatures and persist within the scar, probably to direct its maintenance and remodelling[25,143]. Activated fibroblasts that accumulate late in angiotensin II-induced cardiac hypertrophy also resemble matrifibrocytes[144], suggesting a role for matrifibrocytes in non-ischaemic heart disease, in which perivascular and interstitial fibrosis predominates.

scRNA-seq analyses of other mouse models of heart disease have highlighted the presence of inflammatory, angiogenic and osteogenic fibroblast signatures[82,121,134,137,145,146], which are more abundant with advanced age and might compromise fibroblast–endothelial intercellular signalling[82]. In mice, deletion of *Hif1a* (encoding hypoxia-inducible factor 1α) in fibroblasts leads to excessive fibrosis after MI[132], whereas conditional deletion of *Lats1* and *Lats2* (encoding mechanosensitive Hippo pathway-related serine/threonine protein kinases) in fibroblasts leads to their spontaneous transition to myofibroblasts in uninjured hearts, and formation of a pervasive, non-compacted scar after MI via a mechanism involving the transcription factors YAP and TEAD[121]. Underlining the context-specific effect of the Hippo pathway, epicardial-specific deletion of *Lats1* and *Lats2* in mice was embryonically lethal, leading to defective coronary vasculature remodelling and an impairment in the differentiation of epicardial progenitors into cardiac fibroblasts[121]. scRNA-seq and scATAC-seq analyses in a mouse model of pressure overload, with and without pharmacological inhibition of epigenetic factors, have demonstrated that activated fibroblasts are capable of reverting to quiescent fibroblasts, and MEOX1 was revealed as a key regulator of fibroblast activation[137]. Taken together, these findings show that the annotation of cardiac fibroblast states and inferences of their function is at present more granular in mouse hearts than in human hearts, and that for several mouse cell states, a human equivalent has not yet been identified.

Vascular cell signatures in health and disease

Cardiac vascular cell compartments include those within coronary arteries, capillaries and the endocardium, and have different developmental origins, structures and functions. Importantly, the myocardial microvasculature is the most abundant and capillary endothelial cells are in close contact with cardiomyocytes[147]. Although this microarchitecture infers a close regulatory relationship between endothelial cells and cardiomyocytes, much remains to be understood about the drivers of vascular remodelling in cardiovascular disease.

Endothelial cells

In adult organ donor hearts, the transcriptional signatures of all major cardiac endothelial cell populations have been reported, including capillary, arterial, venous, endocardial and lymphatic endothelial cells[27]. The highest heterogeneity was observed in capillary endothelial cells, which express *RGCC* (encoding a regulator of the cell cycle) and *AQP1* (encoding aquaporin 1) (Fig. 4a), with several new cell states identified.

One of these cell states was characterized by high expression of genes encoding transcription factors (*ATF3*, *FOS* and *JUN*)[148], which could be induced by endoplasmic reticulum stress[149] (as seen in atherosclerosis[150]) and other stimuli such as DNA damage[151] and oxidative stress[152]. A second cell state showed enrichment for cytokine-related genes, such as *CX3CL1*, *CCL2* and *Il16*, and interferon-related genes, suggesting that these cells regulate the local immune response[27]. This analysis remains the most in-depth study of endothelial cell populations, particularly for capillary endothelial cells, with other studies being limited by the numbers of cells and nuclei available, and conservative choices of clustering resolution[33,47]. Indeed, although lymphatic and endocardial endothelial cells have been identified[33,47], the whole range of vascular endothelial cells have not yet been recapitulated[47].

Some of the inconsistencies in endothelial cell states between studies are related to differences in annotations or markers used. For example, the annotation of a *DKK2*$^+$ population[47] probably corresponds to arterial endothelial cells[45]. This example again highlights the importance of standardizing annotations to facilitate more accurate comparison across studies.

SnRNA-seq analysis of patients with DCM have highlighted differences in the transcriptional signatures of venous, capillary and especially endocardial endothelial cells compared with healthy controls[45]. The transforming growth factor-β (TGFβ) signalling pathway is enriched in both venous and capillary endothelial cells[45]. Differential gene expression analysis identified major changes in the endocardium with upregulation of *BMP4* and *BMP6* (encoding bone morphogenetic

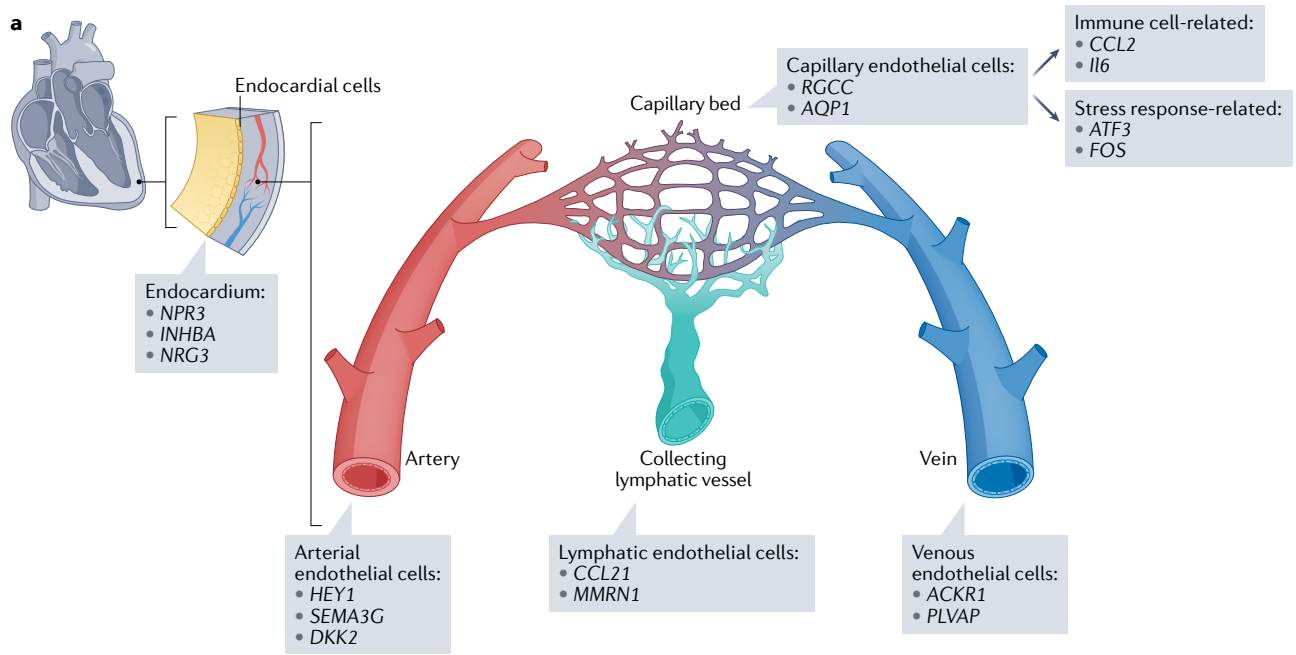

b

	Healthy	
	Human	Mouse
VWF	Capillary, venous and arterial	Endocardium and venous
PLVAP	Venous and endocardium	No cell state specificity
ACKR1	Venous	No cell state specificity
NRG3	Endocardium	Not expressed
NRG1	Low or no expression in endocardium	Endocardium
CCL2	Capillary subset	Low or no expression
ICAM2 (fetal)	Low or no expression	No cell state specificity
RNASE1 (fetal)	No cell state specificity	Low or no expression

c

	DCM	ICM	MI
	Human	Human	Mouse
PLVAP	No reported changes	Induction in capillaries	Upregulation
NRG3	Downregulation in endocardium	No reported changes	No reported changes
NRG1	Upregulation in endocardium	Not investigated	No reported changes
BMP6	Upregulation in endocardium	Not investigated	Not investigated
CCL2	No reported changes	No reported changes	Upregulation on day 3
TGFβ signalling	Upregulation	No reported changes	No reported changes
Proliferation	No reported changes	No reported changes	Upregulation on day 7

Fig. 4 | Species-specific expression of gene markers in endothelial cells of healthy and diseased hearts. a, Illustration of the major vascular structures in the human heart, including the endocardium, and summary of key endothelial cell subsets and their gene markers described in the healthy human heart. **b**, Genes with different expression patterns in endothelial cells of healthy human and mouse hearts. 'No cell state specificity' indicates that the gene is enriched in several cell states without any clear specificity. **c**, Genes with differential expression in endothelial cells in diseased and healthy hearts, including human hearts with dilated cardiomyopathy (DCM) and ischaemic cardiomyopathy (ICM), and mouse hearts after myocardial infarction (MI). TGFβ, transforming growth factor-β.

protein 4 (BMP4) and BMP6, respectively) between healthy hearts and DCM hearts and a shift in expression from *NRG3* (encoding membrane-bound pro-neuregulin 3 (NRG3)) in healthy hearts to *NRG1* in DCM hearts[45,69], which mediates the compensatory response to stress[153,154]. In addition, a genotype stratification study of samples of hearts with DCM and ACM demonstrated that BMP and NRG signalling does not change uniformly in all cardiomyopathies, but that genotype-specific and chamber-specific disruptions of these intercellular signalling pathways are driven by the endocardium[69]. Indeed, in the LV, *NRG1* and *BMP6* are upregulated in the genotypes associated with DCM (variants in *LMNA*, *TTN* or *RBM20*, or no pathogenic variants), but not in ACM (variants in *PKP2*)[69]. However, patients with variants in *PKP2* showed upregulation of *NRG1* and *BMP6* in the RV, whereas patients with no known pathogenic variants did not[69]. Of note, *Nrg1* was described as an endocardial marker in healthy mouse hearts[155], suggesting potential species-specific differences in the role and transcriptional profile of the endocardium (Fig. 4b). By contrast, *NRP3* expression is conserved in both the human and mouse endocardium[28,118,122]. Finally, a potentially angiogenic capillary endothelial cell population that expressed *TMEM163* (encoding transmembrane protein 163) and *KIT* (encoding mast/stem cell growth factor receptor KIT) was shown to increase in both DCM and HCM, suggesting an increase in the formation of small vessels to compensate for impaired cardiac function[47].

In mice, endothelial cells showed increased expression of genes encoding cytokines such as CXCL2 and CCL9 on day 3 after MI, and a proliferative signature on day 7 after MI[156] (Fig. 4c), which was accompanied by an increase in cells enriched for interferon signalling[157]. Upregulation of *Plvap* (encoding plasmalemma vesicle-associated protein (PLVAP), a membrane protein that contributes to permeability) and an increase in endothelial fenestration, stomata of caveolae and transendothelial channel formation was also detected[157]. In human hearts, increased *PLVAP* expression was found in venous endothelial cells and the endocardium, and widespread localization of PLVAP was observed in ischaemic hearts, especially in fibrotic areas[27,157]. Together, these data suggest a potential phenotypic shift in endothelial cells after injury away from the previously described continuous capillary cardiac endothelium[147]. In addition, in a TAC mouse model, scRNA-seq of cadherin 5 lineage-traced cells showed an increase in VEGF, WNT, EGFR and MAPK pathways in a cell state that was enriched for genes related to angiogenesis[158]. Of note, in the adult human heart, expression of *VWF* (encoding von Willebrand factor (vWF)) is detected in most endothelial cell states except lymphatic endothelial cells[27]. By contrast, in the mouse heart, *Vwf* is enriched only in endocardial and venous endothelial cells[155,159] (Fig. 4b). Given the role of vWF in haemostasis, inflammation, vascular permeability and angiogenesis, this finding could have important implications in the interpretation of mouse models of disease for clinical translational purposes[160,161]. Likewise, single-cell and single-nucleus data identified *ACKR1* (encoding a chemokine-scavenging receptor) as a venous endothelial cell marker in the human heart. However, this gene has not been reported in the mouse heart, suggesting a different modulation of chemokine bioavailability and, consequently, leukocyte recruitment across species.

Finally, a single-cell analysis of 4,000 cardiac cells from human fetuses (aged 5–25 weeks) identified four main states of endothelial cells: endocardial, valvular, coronary and vascular[100]. Of note, *CDH11* (encoding cadherin 11) is broadly expressed in human endocardial cells, whereas in equivalent stages of mouse development, its expression is restricted to the endocardium of the valves[64,100]. Expression of *RNASE1* (encoding ribonuclease pancreatic, shown to protect endothelial cells during inflammation[162]) was found in human cardiac fetal endothelial cells only, whereas expression of *Icam2* (encoding intercellular adhesion molecule 2, which is involved in regulating vascular permeability[163]) was specific to the mouse embryo[100] (Fig. 4b). A separate study that analysed 17,000 cardiac from cells human fetuses (aged 19–22 weeks) defined six different endothelial states, including two endocardial populations enriched in *NPR3* (encoding natriuretic peptide receptor 3)[101]. One of these populations co-expressed *INHBA* (encoding inhibin-βa chain, which is selectively expressed in adult endocardium[27,64,100]) and *MEIS2* (encoding meis homeobox 2, a transcriptional regulator essential for cardiac neural crest development[164]). The expression of *MEIS2* might reflect a more immature subset of endocardial cells or a different subset of cells that disappears in adulthood.

Smooth muscle cells and pericytes

SMCs from human adult donor hearts include cells expressing classic gene markers such as *MYH11* and *ACTA2* and a second population with high expression of *CNN1* (encoding calponin 1), which probably represents arterial SMCs[27,165]. Pericyte subtypes include typical *ABCC9*$^+$ and *KCNJ8*$^+$ cells, and a population enriched for *AGT* (encoding angiotensinogen), the expression of which is downregulated in DCM and indicative of dysregulated vasoconstriction[27,45]. scRNA-seq analysis of vascular SMCs (VSMCs) defined a synthetic state enriched in coronary artery SMCs compared with aorta and pulmonary artery SMCs[166], which might indicate a specific adaptation of coronary arteries that are constantly exposed to local pressure changes due to cardiac contraction and relaxation. A proliferative VSMC state expressing *FABP4* (encoding a fatty acid-binding protein) was identified and the numbers were found to be expanded in atherosclerosis[166]. scRNA-seq of atherosclerotic lesions showed that VSMCs undergo phenotypic modulation to transform into unique fibroblast-like cells (fibromyocytes) that contribute to the lesion and fibrous cap in both humans and mice[167]. Loss-of-function and gain-of-function validation studies in mouse models showed that *TCF21* (encoding transcription factor 21) is essential for this phenotypic modulation and that higher levels of *TCF21* are associated with decreased risk of coronary artery disease in humans[167]. Interestingly, in a study of human hearts with DCM or ACM, SMCs and pericytes showed an upregulation in the long non-coding RNA ADAMTS9-AS2 and simultaneous downregulation in *ADAMTS9* (encoding disintegrin and metalloproteinase with thrombospondin motifs 9, which is involved in ECM remodelling)[69]. In addition, genotype-specific changes were also observed. For example, *NOTCH3* (encoding neurogenic locus notch homologue protein 3) was downregulated in the pericytes of patients with pathogenic variants in *TTN* or *PKP2*, whereas *SLIT3* (encoding slit homologue 3 protein, a ligand that regulates fibroblast activity) was upregulated in *ELN*$^+$ SMCs from patients with variants in *PKP2* or *LMNA*[69].

The integration of fate mapping with *Wnt1*–Cre and scRNA-seq helped establish the heterogeneity of cardiac neural crest cell (CNCC)-derived cardiac cell populations from embryonic day (E) 10.5 to postnatal day 7 in mice[168]. As expected, on postnatal day 7, most of the CNCCs localized to the aorta, pulmonary arteries and the coronary vasculature. Nine VSMC populations were identified, in addition to microvascular SMC (mVSMC) and pericyte states. An analysis of lineage trajectories (computational inference of differentiation paths) using RNA velocity revealed a transition from pericytes to mVSMCs with *Notch3*, *Tbx2*, *Fosb* (encoding protein FoxB) and *Klf2* (encoding Krueppel-like factor 2 (KLF2)) as potential key regulators[168–170]. Importantly, when

analysing potential differentiation paths, the inferred latent time based on RNA velocity was similar to the developmental time. The identification of several differentiation paths included one rooted on a *Crabp1*$^+$ (encoding cellular retinoic acid-binding protein 1) cell population, branching into both mesenchymal cells and VSMCs[168], and highlighting previously unknown lineage relationships.

Dynamic adaptations of immune cells

Previous studies have shown that healthy adult human and mouse hearts contain major immune cell populations of both lymphocytes and myeloid cells[27,171]. Resident immune cells, such as cardiac macrophages, are interspersed across the heart between cardiomyocytes, the epicardium, the endocardium, valves and the nodes, where they contribute to organ homeostasis.

Myeloid cells

Myeloid cells in the healthy adult human heart comprise monocytes, dendritic cells and several subtypes of macrophages, such as *LYVE1*$^+$ macrophages (which include MHC-II^{high} and MHC-II^{low} populations), MHC-II$^+$*TREM2*$^+$ macrophages, fibroblast-interacting macrophages and monocyte-derived macrophages[27]. In addition, comparisons with skeletal muscle and kidneys revealed that cardiac myeloid cells, including *LYVE1*$^+$ macrophages, have cardiac-specific features, which might be attributable to the tissue-specific adaptability of myeloid cells[27,31,172]. scRNA-seq findings in mice showed that cardiac macrophages are enriched for ion channels and facilitate electrical conduction through the distal atrioventricular node[173].

Several cardiac monocyte or macrophage populations have been described, with different origins, mechanisms of self-replenishment and distinct functions in the context of inflammation, fibrosis and tissue repair[174–176]. scRNA-seq studies based on mouse models of MI defined a gene expression signature to discriminate a self-renewing macrophage population that originated partly from monocytes (*Ccr2*$^-$MHCII^{high}), in addition to the previously described monocyte-derived macrophages (*Ccr2*$^+$MHC-II^{high}) and self-renewing tissue-resident macrophages (*Ccr2*$^-$MHC-II^{low}*Lyve1*$^+$*Timd4*$^+$)[177,178]. Further analysis revealed a homeostatic and reparative function of tissue-resident macrophages, whereas *Ccr2*$^+$ macrophages are enriched for classic inflammatory pathways[178]. In mouse models, monocytes and monocyte-derived macrophages present at the early stages after MI were found to be recruited via pro-inflammatory circuits[24,177]. Loss-of-function and scRNA-seq studies demonstrated a crucial homeostatic and anti-inflammatory role of tissue-resident macrophages, whereby depletion of these macrophages increased monocyte recruitment and worsened ventricular dysfunction after cardiac injury and hypertension[177–179]. In addition, a putative self-renewing population of tissue-resident macrophages (MHC-II^{low}*Lyve1*$^+$) was shown to contribute to the formation of the lymphatic network in a pressure-overload HF model and during heart development in mice[180,181].

scRNA-seq also revealed immune biphasic cell recruitment in mice after MI[24]. Diffusion map analysis showed a trajectory from early infiltrating monocyte-derived macrophages to inflammatory macrophages, which led to a later peak of tissue-resident reparative macrophages with a pro-regenerative upregulation of *Igf1* (encoding insulin-like growth factor 1)[24]. Combining snRNA-seq and spatial transcriptomics to study samples from patients with MI-induced cardiogenic shock helped to uncover an accumulation of *CCR2*$^+$ macrophages in the injury zone, which predicted the localization of specific fibroblasts and TGFβ2 pathway activity[104]. Specifically, *SPP1*$^+$ (encoding osteopontin) macrophages were enriched in ischaemic tissue samples and colocalized with myofibroblasts, whereas *CCL18*$^+$ macrophages were enriched in fibrotic tissue samples. Finally, in a TAC mouse model, activation of pro-inflammatory macrophages was identified as a key event during the transition from normal to reduced cardiac function[108]. At 5 weeks, macrophages showed upregulation of several chemokines of the CCL subclass, and treating cardiomyocytes in vitro with the conditioned medium of macrophages from the 5-week post-MI samples led to an increase in *Nppa* and *Nppb* expression, typical stress-related genes that are upregulated in HF.

Lymphoid cells

Lymphocytes comprise various subtypes in the healthy adult human heart, including T cell subsets, natural killer (NK) cells and B cells[27]. CD4$^+$ T cells can be classified into naive, effector and regulatory CD4$^+$ T cells, whereas CD8$^+$ T cells include a population of cytotoxic cells characterized by high expression of granzymes and perforin. Cell-mediated cytotoxicity and CD4$^+$ effector T cells have been implicated in the pathogenesis of cardiomyopathy and myocarditis[182–184]. In a snRNA-seq study of HCM and DCM hearts, an increase in lymphocytes expressing *LINGO2* (encoding leucine-rich repeat and immunoglobulin-like domain-containing nogo receptor-interacting protein 2) and several known NK cell markers was identified, but their function remains unclear[47]. NK cells have been shown to have a protective effect against cardiac fibrosis[185], suggesting a potential immune-mediated protective mechanisms during HF. To summarize, enrichment of immune cells before scRNA-seq analysis will help to capture these highly diverse and dynamic cells and improve our understanding of their role in homeostasis and disease.

Functionally important rare cell types

Conduction system and neuronal cells

Neuronal cells represent approximately 1% of human cardiac nuclei and are defined by expression of *NRXN1* (encoding neurexin 1) which is involved in the formation of synaptic contacts[27]. Given that these cells also express *PLP1* (encoding myelin proteolipid protein, a well-known Schwann cell marker), they might plausibly include glial cells or represent doublets of neurons and glial cells[27,186]. In mice, scRNA-seq identified neuronal-like cells based on the expression of *Kcna1* (encoding potassium voltage-gated channel subfamily A member 1) which is involved in regulating nerve signalling[25]. An analysis of 3,961 human cardiac neuronal cells revealed that 80% of these cells are prototypic neurons[27]. Furthermore, a cell state enriched for the WNT signalling receptor gene *LGR5* (encoding leucine-rich repeat-containing G protein coupled receptor 5) and genes encoding myelin constituents was identified as potential Schwann cells[27].

To define the transcriptional signature of the conduction system, specific anatomical regions should be profiled. A multi-species study involving mice, rabbits and cynomolgus monkeys characterized the cells of the mammalian sinoatrial node[187]. *Vsnl1* (encoding the calcium-sensing protein visinin-like protein 1) was defined as a core marker of pacemaker cells in the three species studied. Indeed, disruption of this gene led to reduced beating rates in human induced pluripotent stem cell-derived cardiomyocytes (hiPSC-CMs) and decreased heart rate in mice[187]. Of note, *Kcnj8* was highly expressed in pacemaker cells of cynomolgus monkeys, but not in mice or rabbits. Moreover, analysis of the sinoatrial node from mouse hearts at E16.5 showed that 25% of genes previously reported to be sinoatrial node-specific by bulk RNA sequencing were in fact expressed in cells other than pacemaker cells[188], confirming the value of single-cell approaches[188]. Studying the human

conduction system at the single-cell level is a crucial next step that is currently hampered by limited availability of tissue.

Adipose cells

Adipocytes identified by snRNA-seq analysis using classic markers such as *ADIPOQ* (encoding an adipokine involved in the control of fat metabolism and insulin sensitivity) and *GPAM* (encoding mitochondrial glycerol-3-phosphate acyltransferase 1) represent 0.2–0.5% of the droplets obtained from human hearts[27]. A potential fibrogenic adipocyte precursor expressing ECM-related genes, as well as a cytokine-enriched population were reported; however, the distinction between white and brown cardiac adipocytes cannot yet be made[27]. A disease-specific population of adipocytes identified in DCM and ACM samples is characterized by changes in the expression of genes related to fatty acid metabolism and is enriched in patients with pathogenic variants in *PKP2*, *LMNA* or *RBM20* (ref.[69]). Given the potential role of adipocytes in diseases such as metabolic syndrome and arrhythmia, efforts should be intensified to study this cell population.

Epicardial cells

Epicardial cells are identifiable by their expression of known markers such as *MSLN* and *WT1* (encoding mesothelin and Wilms tumour protein, respectively[27]), and are one of the rarest cell populations in the human heart, thus necessitating enrichment for a full exploration of its complexity. Using a *Wt1* lineage tracing system in a mouse model of MI, two $Wt1^+$ epicardial cell populations were identified, one of which was enriched for *Msln* and keratin-encoding genes, whereas the other was characterized by a proliferation-associated gene signature[43]. Interestingly a $Cd44^+Wt1^-$ epicardial population was also described, suggesting a heterogeneity that goes beyond $Wt1^+$ cells[43]. Furthermore, in a mouse model of neonatal heart regeneration, a combination of scRNA-seq and scATAC-seq analyses revealed an increase in epicardial cells after MI that was accompanied by increased transcriptional activation[155]. Transcription factor motifs were preferentially enriched in *cis*-regulatory elements of epicardial MI-induced genes, including the KLF14 motif specific to the regenerative phase and FOS-related or JUN-related motifs enriched in the non-regenerative phase[155].

Using scRNA-seq, it was possible to assess the cellular heterogeneity of the cardiac crescent in E7.5–E8.0 mouse embryos[66]. Findings from this study led to the identification of a new cardiac field, denoted as the juxtacardiac field, which is characterized by the expression of *Mab21l2*. *Mab21l2* fate mapping showed that the juxtacardiac field contains a pool of progenitor cells for cardiomyocytes and epicardial cells[66]. Although enrichment of rare cell types can be easily achieved in mouse models using lineage tracing tools, in human hearts, it is necessary to select specific anatomical microdomains or identify novel surface markers for prospective sorting.

Cellular networks

Intercellular communication in the heart contributes to development, maintenance of homeostasis and disease progression. Novel computational tools facilitate the mapping of cell states identified using single-cell and single-nucleus transcriptomics integrated with spatial transcriptomics, allowing the unbiased discovery of cellular microenvironments and the prioritization of cell–cell interactions based on niches containing specific cell types or states[90,189] (Fig. 5).

In the adult human heart, CellPhoneDB, a public repository of ligand receptors and their interactions, was used to predict intercellular communications within NOTCH pathways between vascular endothelial cells and VSMCs, uncovering venous-specific and arterial-specific interactions[27]. Furthermore, interactions between fibroblasts and macrophages were predicted, including one that depended on the macrophage migration inhibitory factor (MIF)–CD74 receptor–ligand interaction, which was confirmed by co-expression in spatial transcriptomics[27]. A 2022 study of pressure overload-induced hypertrophy used CellPhoneDB and CellChat to investigate changes in signalling between cardiomyocytes and other cell types[46]. A downregulation in the expression of *EPHB1* and *EFNB2* was observed in cardiomyocytes and endothelial cells, respectively. A validation study using rat cardiomyocytes in 2D cultures and hiPSC-CM organoids with gain-of-function or loss-of-function approaches confirmed that EFNB2–EPHB1 signalling in cardiomyocytes regulates hypertrophy, contraction and stress responses, implicating EPHB1 as a putative therapeutic target in HCM[46]. In a large study of patients with DCM and ACM with different pathogenic variants, an analysis of cell–cell interactions was crucial in identifying genotype and chamber-dependent signalling pathways involved in disease pathogenesis[69]. For example, endothelin signalling originating from the endocardium was increased in the LV of patients with pathogenic variants in *LMNA* and in the RV of patients with pathogenic variants in *PKP2*, but not in patients with other genotypes. Of note, the dynamics of some pathways are cell type-dependent. For example, in the LV of patients with pathogenic variants in *LMNA*, the predicted BMP signalling from SMCs and pericytes to cardiomyocytes is decreased, whereas signalling from endothelial cells to cardiomyocytes is increased[69].

In the adult mouse heart, analysis of non-cardiomyocyte cell populations identified fibroblasts as a crucial intercellular communication hub[22]. After MI, among the non-cardiomyocyte populations, myofibroblasts have the highest number of differentially expressed ligands (consisting mostly of ECM-related genes[24,156]), followed by macrophages[24]. Unexpectedly, endothelial cells express the highest number of differentially expressed receptors, suggesting a role as downstream effectors of paracrine and juxtacrine mechanisms after injury[24,156]. In neonatal mouse hearts, the epicardium was defined as a source of paracrine signalling during both regenerating and non-regenerating phases[155]. As confirmed by in vitro experiments, epicardial induction of *Rspo1* (encoding R-spondin 1, a potent activator of the WNT–β-catenin signalling pathway) is a likely driver of pro-angiogenic signalling. Moreover, given the epicardial upregulation of *Ltbp3* (encoding latent-transforming growth factor-β-binding protein 3 (LTBP3)) and the increased proportion of fibroblasts in the S-phase after treatment with recombinant LTBP3 in vitro, epicardium-derived signalling was suggested to contribute to fibroblast proliferation[155]. Finally, in a TAC mouse model, loss of protective signalling from fibroblasts to cardiomyocytes and increased macrophage–cardiomyocyte interactions were suggested to contribute to the initiation and progression of hypertrophy[24,108,156].

During cardiac development in the human fetus (age 5–25 weeks), a cardiomyocyte-to-endothelial cell BMP paracrine signalling pattern was predicted on the basis of increased cardiomyocyte expression of *BMP5* and *BMP7* and enrichment for BMP receptor genes in endothelial cells, suggesting a potential role for BMP in driving endothelial-to-mesenchymal transition during endocardial cushion formation[100]. In mouse embryonic development, a MIF–CXCR2 interaction was predicted in the second heart field of embryos at E8.5 (ref.[190]). Inhibition of MIF and CXCR2 using small-molecule compounds impaired the elongation of the outflow tract and RV, probably due to defective cell migration. Taken together, to prioritize validation among hundreds of predicted receptor–ligand pairs, filtering criteria require

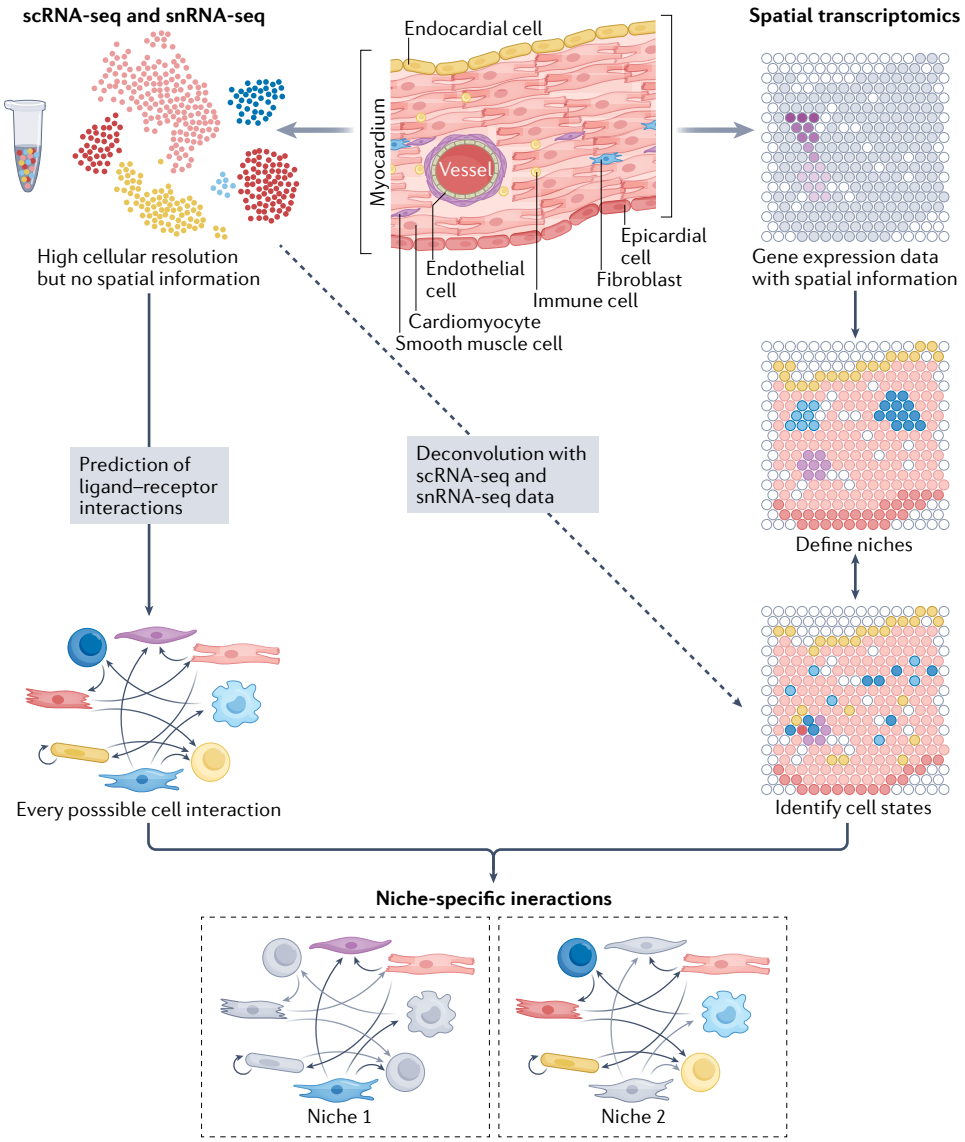

Fig. 5 | Integrating scRNA-seq and snRNA-seq data with spatial transcriptomics analysis to define cellular microenvironments and their dynamic intercellular signalling networks. Single-cell RNA sequencing (scRNA-seq) and single-nucleus RNA sequencing (snRNA-seq) allow the definition of cell states and the prediction of cellular interactions based on the expression of genes encoding ligands and receptors. However, these data do not provide information about cellular proximity. Spatial transcriptomics allows the mapping of gene expression within tissue sections across microtiles that represent microbulk transcriptomics data. By mapping scRNA-seq and snRNA-seq data onto spatial data using computational tools such as cell2location and Giotto, it is possible to predict the localization of cell types and states within microtiles and microanatomical niches. The cellular proximity within the defined cellular niches facilitates inferences on the most probable cellular interactions and the identification of putative functional microenvironments.

computational tools, which take into consideration the activation of downstream cascades in the cells receiving the signalling cues[90,189].

Future directions for omics approaches

Transforming diagnosis and therapy

Single-cell, single-nucleus and spatial transcriptomics accompanied by machine learning-based analysis is likely to contribute to the identification of markers for diagnostic and prognostic evaluation of cardiovascular diseases. In particular, these technologies can provide new insights into cell states (including those of rare cells) and cell-type composition of diseased hearts, and define cell-specific theraputic targets[45,46,191]. An early scRNA-seq study identified the source of IL-11, a novel anti-fibrotic target for the cardiovascular system[145], demonstrating the potential of single-cell omics approaches in developing innovative therapies.

Capturing the earliest and most specific therapeutic cellular targets among the numerous maladaptive cardiomyocyte responses driving HF is crucial in hereditary DCM compared with HCM, in which

variants in the same culprit gene can lead to opposite phenotypes[192]. Although a study of patients with end-stage HCM or DCM showed changes in cellular composition across the two groups, only minimal differences were detected at the transcriptional level[47], highlighting a need to stratify patients on the basis of aetiology and to study earlier stages of disease progression. Indeed, analysis of genotype-stratified DCM samples identified specific transcriptional changes in different pathogenic variants groups, in addition to shared gene signatures. The number of differentially expressed genes was sufficient to develop a deep learning method that could predict the genotype on the basis of gene expression signatures of cardiomyocytes, endothelial cells, fibroblasts and myeloid cells[69]. This finding indicates that even at later stages of HF, the underlying cellular landscape and implicitly maladaptive mechanisms differ depending on the underlying cause. To understand the mechanisms involved in progression of DCM to HF, multimodal omics analysis should be performed in both early and late phases of disease, and patients should be stratified according to disease aetiology. Likewise, in ICM, understanding the cellular changes occurring before the onset of HF will be crucial to the stratification of patients in minimizing the current heterogeneity in response to therapy and towards personalized medicine approaches. Taken together, such information can improve our understanding of the pathobiological mechanisms underlying HF and guide the identification of prognostic biomarkers and novel druggable targets for cell-targeted interceptive medicine[193].

hiPSC-derived cardiovascular cells

HiPSC-derived cardiovascular cells and cardiovascular cells derived from direct reprogramming hold great promise, not only for cardiovascular regeneration but also for drug screening and disease modelling, which is especially relevant for cardiomyocytes, given the lack of reliable cell lines and the challenges in working with large numbers of primary cells for an extended amount of time. To ensure the replicability of hiPSC-CMs as in vitro models, the maturation process needs to be improved and the phenotypic heterogeneity of the cells needs to be functionally evaluated. This latter step is necessary to establish precise models of the cellular subtypes identified in vivo by single-cell and single-nucleus approches. Indeed some of these cell states might be better therapeutic targets than others or even therapeutic products for cell therapy. The integration of single-cell and single-nucleus transcriptomics data from human hearts from all stages of development with those from hiPSC-derived cardiovascular cells contributes to our understanding of the variability in differentiation and maturity occurring in vitro compared with the processes occurring within the cardiac cellular landscape in vivo[124,194–198]. One such study described the role of the progesterone receptor in driving sex-specific metabolic programmes and maturation of cardiomyocytes[199]. Importantly, transcriptomics and epigenomic single-cell analyses have guided improvements in protocols for differentiation and maturation of cardiovascular lineages such as cardiomyocytes and endothelial cells in hiPSC-based 2D and 3D platforms, as well as in direct reprogramming approaches[38,200–203]. Furthermore, single-cell studies of hiPSC-derived cardiovascular cells were not only highly informative in reproducing the differentiation steps occurring in cardiac development, but also contributed to the modelling of congenital and other genetic disorders[194,204–206]. Such studies provide a comprehensive overview of the transcriptional changes that occur in specific cells at various stages of differentiation to facilitate precise mechanistic insights, as seen in studies showing a dosage-dependent effect of TBX5 in different cell states in the setting of congenital heart disease, as well as the convergence of cell cycle dysregualtion and autophagy as pathogenic mechanisms of hypoplastic heart disease[204,207].

Age, sex and comorbidities

As presented throughout this Review, great effort has already been made to understand the complexity of the cardiac cellular landscape. However, some knowledge gaps remain. An urgent need exists for the development of a longitudinal heart atlas from the tissues of infants, children, adolescents and young adults (aged 20–40 years) that recapitulates the substantial morphological and haemodynamic changes occurring from birth until adulthood. Understanding sex-related differences in health and disease is a developing area in cardiology. A single-cell study showed differences in the prevalence of fibroblast subtypes and gene expression patterns between male and female mice[22,144] and between inbred strains[25]. Furthermore, a study based on limited numbers of donor hearts identified the progesterone receptor as a key mediator of sex-dependent transcriptional programmes during cardiomyocyte maturation[199]. Therefore, given the effect of biological variables such as sex and ancestry on cardiovascular risk, it is imperative to integrate datasets from increasing numbers of donors to evaluate the influence of these variables on the human cardiac cellular landscape. Moreover, patients with cardiovascular disease, especially those of advanced age, often have comorbidities such diabetes mellitus, obesity and high blood pressure, which will need to be considered in the analysis and interpretation. The stratification of patients and organ donors will be possible through the integration of data from hundreds of individuals and the collection of appropriate clinical metadata.

Conclusions

Single-cell and single-nucleus omics technologies have provided invaluable novel insights into the cardiac cellular landscape to facilitate a better understanding of disease mechanisms and more tools for accurate risk stratification and precision medicine. However, newly defined cell states not only require thorough validation, but also cooperative and interdisciplinary efforts to standardize definitions and nomenclature within and across species, which will facilitate more accurate comparison between studies and the optimization of experimental designs for disease models. Finally, an urgent need exists to ensure the availability of computational resources and training for the new generation of scientists and clinicians, to allow improved interrogation of the biology and to accelerate the application of these transformative technologies to the study and treatment of cardiac disease.

Published online: 20 December 2022

References

1. Morton, S. U., Quiat, D., Seidman, J. G. & Seidman, C. E. Genomic frontiers in congenital heart disease. *Nat. Rev. Cardiol.* **19**, 26–42 (2022).
2. Banjo, T. et al. Haemodynamically dependent valvulogenesis of zebrafish heart is mediated by flow-dependent expression of miR-21. *Nat. Commun.* **4**, 1978 (2013).
3. van Heesch, S. et al. The translational landscape of the human heart. *Cell* https://doi.org/10.1016/j.cell.2019.05.010 (2019).
4. Saucerman, J. J., Tan, P. M., Buchholz, K. S., McCulloch, A. D. & Omens, J. H. Mechanical regulation of gene expression in cardiac myocytes and fibroblasts. *Nat. Rev. Cardiol.* **16**, 361–378 (2019).
5. Liu, Y. et al. RNA-Seq identifies novel myocardial gene expression signatures of heart failure. *Genomics* **105**, 83–89 (2015).
6. Burke, M. A. et al. Molecular profiling of dilated cardiomyopathy that progresses to heart failure. *JCI Insight* https://doi.org/10.1172/jci.insight.86898 (2016).
7. Nomura, S. et al. Cardiomyocyte gene programs encoding morphological and functional signatures in cardiac hypertrophy and failure. *Nat. Commun.* **9**, 4435 (2018).
8. Roth, G. A. et al. Global burden of cardiovascular diseases and risk factors, 1990–2019: update from the GBD 2019 study. *J. Am. Coll. Cardiol.* **76**, 2982–3021 (2020).

9. Groenewegen, A., Rutten, F. H., Mosterd, A. & Hoes, A. W. Epidemiology of heart failure. *Eur. J. Heart Fail.* **22**, 1342–1356 (2020).
10. Murphy, S. P., Ibrahim, N. E. & Januzzi, J. L. Jr. Heart failure with reduced ejection fraction: a review. *JAMA* **324**, 488–504 (2020).
11. Maddox, T. M. et al. 2021 Update to the 2017 ACC expert consensus decision pathway for optimization of heart failure treatment: answers to 10 pivotal issues about heart failure with reduced ejection fraction a report of the American College of Cardiology Solution Set Oversight Committee. *J. Am. Coll. Cardiol.* **77**, 772–810 (2021).
12. Aldridge, S. & Teichmann, S. A. Single cell transcriptomics comes of age. *Nat. Commun.* **11**, 4307 (2020).
13. Domínguez Conde, C. et al. Cross-tissue immune cell analysis reveals tissue-specific adaptations and clonal architecture in humans. *Science* **376**, eabl5197 (2022).
14. Pasquini, G., Rojo Arias, J. E., Schafer, P. & Busskamp, V. Automated methods for cell type annotation on scRNA-seq data. *Comput. Struct. Biotechnol. J.* **19**, 961–969 (2021).
15. Clarke, Z. A. et al. Tutorial: guidelines for annotating single-cell transcriptomic maps using automated and manual methods. *Nat. Protoc.* **16**, 2749 (2021).
16. Efremova, M., Vento-Tormo, M., Teichmann, S. A. & Vento-Tormo, R. CellPhoneDB: inferring cell-cell communication from combined expression of multi-subunit ligand-receptor complexes. *Nat. Protoc.* **15**, 1484–1506 (2020).
17. Jin, S. Q. et al. Inference and analysis of cell-cell communication using CellChat. *Nat. Commun.* https://doi.org/10.1038/s41467-021-21246-9 (2021).
18. Svensson, V., Vento-Tormo, R. & Teichmann, S. A. Exponential scaling of single-cell RNA-seq in the past decade. *Nat. Protoc.* **13**, 599–604 (2018).
19. Efremova, M. & Teichmann, S. A. Computational methods for single-cell omics across modalities. *Nat. Methods* **17**, 14–17 (2020).
20. Paik, D. T., Cho, S., Tian, L., Chang, H. Y. & Wu, J. C. Single-cell RNA sequencing in cardiovascular development, disease and medicine. *Nat. Rev. Cardiol.* **17**, 457–473 (2020).
21. Cossarizza, A. et al. Guidelines for the use of flow cytometry and cell sorting in immunological studies (second edition). *Eur. J. Immunol.* **49**, 1457–1973 (2019).
22. Skelly, D. A. et al. Single-cell transcriptional profiling reveals cellular diversity and intercommunication in the mouse heart. *Cell Rep.* **22**, 600–610 (2018).
23. DeLaughter, D. M. et al. Single-cell resolution of temporal gene expression during heart development. *Dev. Cell* **39**, 480–490 (2016).
24. Farbehi, N. et al. Single-cell expression profiling reveals dynamic flux of cardiac stromal, vascular and immune cells in health and injury. *Elife* https://doi.org/10.7554/eLife.43882 (2019).
25. Forte, E. et al. Dynamic interstitial cell response during myocardial infarction predicts resilience to rupture in genetically diverse mice. *Cell Rep.* **30**, 3149–3163.e6 (2020).
26. Tombor, L. S. et al. Single cell sequencing reveals endothelial plasticity with transient mesenchymal activation after myocardial infarction. *Nat. Commun.* **12**, 681 (2021).
27. Litvinukova, M. et al. Cells of the adult human heart. *Nature* **588**, 466–472 (2020).
28. Gladka, M. M. et al. Single-cell sequencing of the healthy and diseased heart reveals cytoskeleton-associated protein 4 as a new modulator of fibroblasts activation. *Circulation* **138**, 166–180 (2018).
29. Molenaar, B. et al. Single-cell transcriptomics following ischemic injury identifies a role for B2M in cardiac repair. *Commun. Biol.* **4**, 146 (2021).
30. Kannan, S. et al. Large particle fluorescence-activated cell sorting enables high-quality single-cell RNA sequencing and functional analysis of adult cardiomyocytes. *Circ. Res.* **125**, 567–569 (2019).
31. Eraslan, G. et al. Single-nucleus cross-tissue molecular reference maps toward understanding disease gene function. *Science* **376**, eabl4290 (2022).
32. Tucker, N. R. et al. Myocyte-specific upregulation of ACE2 in cardiovascular disease: implications for SARS-CoV-2-mediated myocarditis. *Circulation* **142**, 708–710 (2020).
33. Tucker, N. R. et al. Transcriptional and cellular diversity of the human heart. *Circulation* **142**, 466–482 (2020).
34. See, K. et al. Single cardiomyocyte nuclear transcriptomes reveal a lincRNA-regulated de-differentiation and cell cycle stress-response in vivo. *Nat. Commun.* **8**, 225 (2017).
35. Nicin, L. et al. Single nuclei sequencing reveals novel insights into the regulation of cellular signatures in children with dilated cardiomyopathy. *Circulation* **143**, 1704–1719 (2021).
36. Hu, P. et al. Single-nucleus transcriptomic survey of cell diversity and functional maturation in postnatal mammalian hearts. *Genes Dev.* **32**, 1344–1357 (2018).
37. Nadelmann, E. R. et al. Isolation of nuclei from mammalian cells and tissues for single-nucleus molecular profiling. *Curr. Protoc.* **1**, e132 (2021).
38. Selewa, A. et al. Systematic comparison of high-throughput single-cell and single-nucleus transcriptomes during cardiomyocyte differentiation. *Sci. Rep.* **10**, 1535 (2020).
39. Denisenko, E. et al. Systematic assessment of tissue dissociation and storage biases in single-cell and single-nucleus RNA-seq workflows. *Genome Biol.* **21**, 130 (2020).
40. Rodrigues, E. C., Grawenhoff, J., Baumann, S. J., Lorenzon, N. & Maurer, S. P. Mammalian neuronal mRNA transport complexes: the few knowns and the many unknowns. *Front. Integr. Neurosci.* **15**, 692948 (2021).
41. Ivanovitch, K. et al. Ventricular, atrial, and outflow tract heart progenitors arise from spatially and molecularly distinct regions of the primitive streak. *PLoS Biol.* **19**, e3001200 (2021).
42. Lescroart, F. et al. Defining the earliest step of cardiovascular lineage segregation by single-cell RNA-seq. *Science* **359**, 1177–1181 (2018).
43. Hesse, J. et al. Single-cell transcriptomics defines heterogeneity of epicardial cells and fibroblasts within the infarcted murine heart. *Elife* https://doi.org/10.7554/eLife.65921 (2021).
44. Axelsson Raja, A. et al. Ablation of lysophosphatidic acid receptor 1 attenuates hypertrophic cardiomyopathy in a mouse model. *Proc. Natl Acad. Sci. USA* **119**, e2204174119 (2022).
45. Koenig, A. L. et al. Single-cell transcriptomics reveals cell-type-specific diversification in human heart failure. *Nat. Cardiovasc. Res.* **1**, 263–280 (2022).
46. Nicin, L. et al. A human cell atlas of the pressure-induced hypertrophic heart. *Nat. Cardiovasc. Res.* **1**, 174–185 (2022).
47. Chaffin, M. et al. Single-nucleus profiling of human dilated and hypertrophic cardiomyopathy. *Nature* https://doi.org/10.1038/s41586-022-04817-8 (2022).
48. Cui, M. et al. Dynamic transcriptional responses to injury of regenerative and non-regenerative cardiomyocytes revealed by single-nucleus RNA sequencing. *Dev. Cell* **53**, 102–116.e8 (2020).
49. Koda, M. et al. Nuclear hypertrophy reflects increased biosynthetic activities in myocytes of human hypertrophic hearts. *Circ. J.* **70**, 710–718 (2006).
50. Chongtham, M. C., Todorov, H., Wettschereck, J. E., Gerber, S. & Winter, J. Isolation of nuclei and downstream processing of cell-type-specific nuclei from micro-dissected mouse brain regions – techniques and caveats. *bioRxiv* https://doi.org/10.1101/2020.11.18.374223 (2020).
51. Cui, M. & Olson, E. N. Protocol for single-nucleus transcriptomics of diploid and tetraploid cardiomyocytes in murine hearts. *STAR Protoc.* **1**, 100049 (2020).
52. Wojcik, K. & Dobrucki, J. W. Interaction of a DNA intercalator DRAQ5, and a minor groove binder SYTO17, with chromatin in live cells – influence on chromatin organization and histone–DNA interactions. *Cytom. A* **73**, 555–562 (2008).
53. Chongtham, M. C., Butto, T., Mungikar, K., Gerber, S. & Winter, J. INTACT vs. FANS for cell-type-specific nuclei sorting: a comprehensive qualitative and quantitative comparison. *Int. J. Mol. Sci.* https://doi.org/10.3390/ijms22105335 (2021).
54. Zhang, X. et al. Comparative analysis of droplet-based ultra-high-throughput single-cell RNA-seq systems. *Mol. Cell* **73**, 130–142.e5 (2019).
55. Kolodziejczyk, A. A., Kim, J. K., Svensson, V., Marioni, J. C. & Teichmann, S. A. The technology and biology of single-cell RNA sequencing. *Mol. Cell* **58**, 610–620 (2015).
56. Macosko, E. Z. et al. Highly parallel genome-wide expression profiling of individual cells using nanoliter droplets. *Cell* **161**, 1202–1214 (2015).
57. Zheng, G. X. et al. Massively parallel digital transcriptional profiling of single cells. *Nat. Commun.* **8**, 14049 (2017).
58. Hagemann-Jensen, M. et al. Single-cell RNA counting at allele and isoform resolution using Smart-seq3. *Nat. Biotechnol.* **38**, 708–714 (2020).
59. Hagemann-Jensen, M., Ziegenhain, C. & Sandberg, R. Scalable single-cell RNA sequencing from full transcripts with Smart-seq3xpress. *Nat. Biotechnol.* https://doi.org/10.1038/s41587-022-01311-4 (2022).
60. Yekelchyk, M., Guenther, S., Preussner, J. & Braun, T. Mono- and multi-nucleated ventricular cardiomyocytes constitute a transcriptionally homogenous cell population. *Basic. Res. Cardiol.* **114**, 36 (2019).
61. Wang, Y. et al. Single-cell analysis of murine fibroblasts identifies neonatal to adult switching that regulates cardiomyocyte maturation. *Nat. Commun.* **11**, 2585 (2020).
62. Wang, L. et al. Single-cell reconstruction of the adult human heart during heart failure and recovery reveals the cellular landscape underlying cardiac function. *Nat. Cell Biol.* **22**, 108–119 (2020).
63. Rosenberg, A. B. et al. Single-cell profiling of the developing mouse brain and spinal cord with split-pool barcoding. *Science* **360**, 176–182 (2018).
64. Xu, K. et al. Cell-type transcriptome atlas of human aortic valves reveal cell heterogeneity and endothelial to mesenchymal transition involved in calcific aortic valve disease. *Arterioscler. Thromb. Vasc. Biol.* **40**, 2910–2921 (2020).
65. Pirruccello, J. P. et al. Deep learning enables genetic analysis of the human thoracic aorta. *Nat. Genet.* **54**, 40–51 (2022).
66. Tyser, R. C. V. et al. Characterization of a common progenitor pool of the epicardium and myocardium. *Science* https://doi.org/10.1126/science.abb2986 (2021).
67. Davis, A., Gao, R. & Navin, N. E. SCOPIT: sample size calculations for single-cell sequencing experiments. *BMC Bioinformatics* **20**, 566 (2019).
68. Schmid, K. T. et al. scPower accelerates and optimizes the design of multi-sample single cell transcriptomic studies. *Nat. Commun.* **12**, 6625 (2021).
69. Reichart, D. et al. Pathogenic variants damage cell composition and single cell transcription in cardiomyopathies. *Science* **377**, eabo1984 (2022).
70. Luecken, M. D. & Theis, F. J. Current best practices in single-cell RNA-seq analysis: a tutorial. *Mol. Syst. Biol.* **15**, e8746 (2019).
71. Azizi, E. et al. Single-cell map of diverse immune phenotypes in the breast tumor microenvironment. *Cell* **174**, 1293–1308.e36 (2018).
72. Parekh, S., Ziegenhain, C., Vieth, B., Enard, W. & Hellmann, I. zUMIs – a fast and flexible pipeline to process RNA sequencing data with UMIs. *Gigascience* https://doi.org/10.1093/gigascience/giy059 (2018).
73. Ilicic, T. et al. Classification of low quality cells from single-cell RNA-seq data. *Genome Biol.* **17**, 29 (2016).
74. Fleming, S. J. et al. Unsupervised removal of systematic background noise from droplet-based single-cell experiments using CellBender. *bioRxiv* https://doi.org/10.1101/791699 (2022).
75. Young, M. D. & Behjati, S. SoupX removes ambient RNA contamination from droplet-based single-cell RNA sequencing data. *Gigascience* https://doi.org/10.1093/gigascience/giaa151 (2020).
76. Yang, S. et al. Decontamination of ambient RNA in single-cell RNA-seq with DecontX. *Genome Biol.* **21**, 57 (2020).

77. Osorio, D. & Cai, J. J. Systematic determination of the mitochondrial proportion in human and mice tissues for single-cell RNA-sequencing data quality control. *Bioinformatics* **37**, 963–967 (2021).
78. Wolock, S. L., Lopez, R. & Klein, A. M. Scrublet: computational identification of cell doublets in single-cell transcriptomic data. *Cell Syst.* **8**, 281–291.e9 (2019).
79. Bernstein, N. J. et al. Solo: doublet identification in single-cell RNA-seq via semi-supervised deep learning. *Cell Syst.* **11**, 95–101.e5 (2020).
80. Luecken, M. D. et al. Benchmarking atlas-level data integration in single-cell genomics. *Nat. Methods* **19**, 41–50 (2022).
81. Tran, H. T. N. et al. A benchmark of batch-effect correction methods for single-cell RNA sequencing data. *Genome Biol.* **21**, 12 (2020).
82. Vidal, R. et al. Transcriptional heterogeneity of fibroblasts is a hallmark of the aging heart. *JCI Insight* https://doi.org/10.1172/jci.insight.131092 (2019).
83. Miao, Z. et al. Putative cell type discovery from single-cell gene expression data. *Nat. Methods* **17**, 621–628 (2020).
84. Liu, S., Thennavan, A., Garay, J. P., Marron, J. S. & Perou, C. M. MultiK: an automated tool to determine optimal cluster numbers in single-cell RNA sequencing data. *Genome Biol.* **22**, 232 (2021).
85. Kimmel, J. C. & Kelley, D. R. Semisupervised adversarial neural networks for single-cell classification. *Genome Res.* **31**, 1781–1793 (2021).
86. Lotfollahi, M. et al. Mapping single-cell data to reference atlases by transfer learning. *Nat. Biotechnol.* **40**, 121–130 (2022).
87. Jain, M. S. et al. MultiMAP: dimensionality reduction and integration of multimodal data. *Genome Biol.* **22**, 346 (2021).
88. Gayoso, A. et al. Joint probabilistic modeling of single-cell multi-omic data with totalVI. *Nat. Methods* **18**, 272–282 (2021).
89. Ashuach, T., Gabitto, M. I., Jordan, M. I. & Yosef, N. MultiVI: deep generative model for the integration of multi-modal data. *bioRxiv* https://doi.org/10.1101/2021.08.20.457057 (2021).
90. Kleshchevnikov, V. et al. Cell2location maps fine-grained cell types in spatial transcriptomics. *Nat. Biotechnol.* https://doi.org/10.1038/s41587-021-01139-4 (2022).
91. Andersson, A. et al. Single-cell and spatial transcriptomics enables probabilistic inference of cell type topography. *Commun. Biol.* **3**, 565 (2020).
92. Dries, R. et al. Giotto: a toolbox for integrative analysis and visualization of spatial expression data. *Genome Biol.* **22**, 78 (2021).
93. Stahl, P. L. et al. Visualization and analysis of gene expression in tissue sections by spatial transcriptomics. *Science* **353**, 78–82 (2016).
94. Rodriques, S. G. et al. Slide-seq: a scalable technology for measuring genome-wide expression at high spatial resolution. *Science* **363**, 1463–1467 (2019).
95. Merritt, C. R. et al. Multiplex digital spatial profiling of proteins and RNA in fixed tissue. *Nat. Biotechnol.* **38**, 586–599 (2020).
96. Sikkema, L. et al. An integrated cell atlas of the human lung in health and disease. *bioRxiv* https://doi.org/10.1101/2022.03.10.483747 (2022).
97. Tabula Sapiens, C. et al. The Tabula Sapiens: a multiple-organ, single-cell transcriptomic atlas of humans. *Science* **376**, eabl4896 (2022).
98. Elmentaite, R., Dominguez Conde, C., Yang, L. & Teichmann, S. A. Single-cell atlases: shared and tissue-specific cell types across human organs. *Nat. Rev. Genet.* **23**, 395–410 (2022).
99. Nielles-Vallespin, S. et al. Cardiac diffusion: technique and practical applications. *J. Magn. Reson. Imaging* **52**, 348–368 (2020).
100. Cui, Y. et al. Single-cell transcriptome analysis maps the developmental track of the human heart. *Cell Rep.* **26**, 1934–1950.e5 (2019).
101. Suryawanshi, H. et al. Cell atlas of the foetal human heart and implications for autoimmune-mediated congenital heart block. *Cardiovasc. Res.* **116**, 1446–1457 (2020).
102. Li, G. et al. Transcriptomic profiling maps anatomically patterned subpopulations among single embryonic cardiac cells. *Dev. Cell* **39**, 491–507 (2016).
103. Xiao, Y. et al. Hippo signaling plays an essential role in cell state transitions during cardiac fibroblast development. *Dev. Cell* **45**, 153–169.e6 (2018).
104. Kuppe, C. et al. Spatial multi-omic map of human myocardial infarction. *Nature* **608**, 766–777 (2022).
105. Piroddi, N. et al. Myocardial overexpression of ANKRD1 causes sinus venosus defects and progressive diastolic dysfunction. *Cardiovasc. Res.* **116**, 1458–1472 (2020).
106. Sergeeva, I. A. & Christoffels, V. M. Regulation of expression of atrial and brain natriuretic peptide, biomarkers for heart development and disease. *Biochim. Biophys. Acta* **1832**, 2403–2413 (2013).
107. Sergeeva, I. A. et al. A transgenic mouse model for the simultaneous monitoring of ANF and BNP gene activity during heart development and disease. *Cardiovasc. Res.* **101**, 78–86 (2014).
108. Ren, Z. et al. Single-cell reconstruction of progression trajectory reveals intervention principles in pathological cardiac hypertrophy. *Circulation* **141**, 1704–1719 (2020).
109. Hill, M. C. et al. Integrated multi-omic characterization of congenital heart disease. *Nature* **608**, 181–191 (2022).
110. Riching, A. S. & Song, K. Cardiac regeneration: new insights into the frontier of ischemic heart failure therapy. *Front. Bioeng. Biotechnol.* **8**, 637538 (2020).
111. Honkoop, H. et al. Single-cell analysis uncovers that metabolic reprogramming by ErbB2 signaling is essential for cardiomyocyte proliferation in the regenerating heart. *Elife* https://doi.org/10.7554/eLife.50163 (2019).
112. Frangogiannis, N. G. Cardiac fibrosis. *Cardiovasc. Res.* **117**, 1450–1488 (2021).
113. Aghajanian, H. et al. Targeting cardiac fibrosis with engineered T cells. *Nature* **573**, 430–433 (2019).
114. Duan, Q. et al. BET bromodomain inhibition suppresses innate inflammatory and profibrotic transcriptional networks in heart failure. *Sci. Transl. Med.* https://doi.org/10.1126/scitranslmed.aah5084 (2017).
115. Fang, L., Murphy, A. J. & Dart, A. M. A clinical perspective of anti-fibrotic therapies for cardiovascular disease. *Front. Pharmacol.* **8**, 186 (2017).
116. Gourdie, R. G., Dimmeler, S. & Kohl, P. Novel therapeutic strategies targeting fibroblasts and fibrosis in heart disease. *Nat. Rev. Drug Discov.* **15**, 620–638 (2016).
117. Rog-Zielinska, E. A., Norris, R. A., Kohl, P. & Markwald, R. The living scar – cardiac fibroblasts and the injured heart. *Trends Mol. Med.* **22**, 99–114 (2016).
118. Luo, S. et al. SAIL: a new conserved anti-fibrotic lncRNA in the heart. *Basic Res. Cardiol.* **116**, 15 (2021).
119. Pinto, A. R. et al. Revisiting cardiac cellular composition. *Circ. Res.* **118**, 400–409 (2016).
120. Soliman, H. et al. Multipotent stromal cells: one name, multiple identities. *Cell Stem Cell* **28**, 1690–1707 (2021).
121. Xiao, Y. et al. Hippo pathway deletion in adult resting cardiac fibroblasts initiates a cell state transition with spontaneous and self-sustaining fibrosis. *Genes Dev.* **33**, 1491–1505 (2019).
122. Rao, M. et al. Resolving the intertwining of inflammation and fibrosis in human heart failure at single-cell level. *Basic Res. Cardiol.* **116**, 55 (2021).
123. Sim, W. S., Park, B. W., Ban, K. & Park, H. J. In situ preconditioning of human mesenchymal stem cells elicits comprehensive cardiac repair following myocardial infarction. *Int. J. Mol. Sci.* https://doi.org/10.3390/ijms22031449 (2021).
124. McCracken, I. R. et al. Lack of evidence of angiotensin-converting enzyme 2 expression and replicative infection by SARS-CoV-2 in human endothelial cells. *Circulation* **143**, 865–868 (2021).
125. Brener, M. I. et al. Clinico-histopathologic and single-nuclei RNA-sequencing insights into cardiac injury and microthrombi in critical COVID-19. *JCI Insight* https://doi.org/10.1172/jci.insight.154633 (2022).
126. Zou, X. et al. Single-cell RNA-seq data analysis on the receptor ACE2 expression reveals the potential risk of different human organs vulnerable to 2019-nCoV infection. *Front. Med.* **14**, 185–192 (2020).
127. Muus, C. et al. Single-cell meta-analysis of SARS-CoV-2 entry genes across tissues and demographics. *Nat. Med.* **27**, 546–559 (2021).
128. Sungnak, W. et al. SARS-CoV-2 entry factors are highly expressed in nasal epithelial cells together with innate immune genes. *Nat. Med.* **26**, 681–687 (2020).
129. Delorey, T. M. et al. COVID-19 tissue atlases reveal SARS-CoV-2 pathology and cellular targets. *Nature* **595**, 107–113 (2021).
130. Buechler, M. B. et al. Cross-tissue organization of the fibroblast lineage. *Nature* **593**, 575–579 (2021).
131. Chong, J. J. et al. Adult cardiac-resident MSC-like stem cells with a proepicardial origin. *Cell Stem Cell* **9**, 527–540 (2011).
132. Janbandhu, V. et al. Hif-1a suppresses ROS-induced proliferation of cardiac fibroblasts following myocardial infarction. *Cell Stem Cell* **29**, 281–297.e12 (2022).
133. Noseda, M. et al. PDGFRα demarcates the cardiogenic clonogenic Sca1+ stem/progenitor cell in adult murine myocardium. *Nat. Commun.* **6**, 6930 (2015).
134. Soliman, H. et al. Pathogenic potential of hic1-expressing cardiac stromal progenitors. *Cell Stem Cell* **26**, 205–220.e8 (2020).
135. Soliman, H. & Rossi, F. M. V. Cardiac fibroblast diversity in health and disease. *Matrix Biol.* **91-92**, 75–91 (2020).
136. Pillai, I. C. L. et al. Cardiac fibroblasts adopt osteogenic fates and can be targeted to attenuate pathological heart calcification. *Cell Stem Cell* **20**, 218–232.e5 (2017).
137. Alexanian, M. et al. A transcriptional switch governs fibroblast activation in heart disease. *Nature* **595**, 438–443 (2021).
138. Zhang, Q. J. et al. Matricellular protein cilp1 promotes myocardial fibrosis in response to myocardial infarction. *Circ. Res.* **129**, 1021–1035 (2021).
139. Meyer, I. S. et al. The cardiac microenvironment uses non-canonical WNT signaling to activate monocytes after myocardial infarction. *EMBO Mol. Med.* **9**, 1279–1293 (2017).
140. Saxena, A. et al. IL-1 induces proinflammatory leukocyte infiltration and regulates fibroblast phenotype in the infarcted myocardium. *J. Immunol.* **191**, 4838–4848 (2013).
141. Abe, H. et al. NF-κB activation in cardiac fibroblasts results in the recruitment of inflammatory Ly6C(hi) monocytes in pressure-overloaded hearts. *Sci. Signal.* **14**, eabe4932 (2021).
142. Tallquist, M. D. & Molkentin, J. D. Redefining the identity of cardiac fibroblasts. *Nat. Rev. Cardiol.* **14**, 484–491 (2017).
143. Fu, X. et al. Specialized fibroblast differentiated states underlie scar formation in the infarcted mouse heart. *J. Clin. Invest.* **128**, 2127–2143 (2018).
144. McLellan, M. A. et al. High-resolution transcriptomic profiling of the heart during chronic stress reveals cellular drivers of cardiac fibrosis and hypertrophy. *Circulation* **142**, 1448–1463 (2020).
145. Schafer, S. et al. IL-11 is a crucial determinant of cardiovascular fibrosis. *Nature* **552**, 110–115 (2017).
146. Ruiz-Villalba, A. et al. Single-cell RNA sequencing analysis reveals a crucial role for CTHRC1 (collagen triple helix repeat containing 1) cardiac fibroblasts after myocardial infarction. *Circulation* **142**, 1831–1847 (2020).

147. Aird, W. C. Phenotypic heterogeneity of the endothelium: II. Representative vascular beds. *Circ. Res.* **100**, 174–190 (2007).
148. Hai, T. & Curran, T. Cross-family dimerization of transcription factors Fos/Jun and ATF/CREB alters DNA binding specificity. *Proc. Natl Acad. Sci. USA* **88**, 3720–3724 (1991).
149. Jiang, H. Y. et al. Activating transcription factor 3 is integral to the eukaryotic initiation factor 2 kinase stress response. *Mol. Cell Biol.* **24**, 1365–1377 (2004).
150. Nawa, T. et al. Expression of transcriptional repressor ATF3/LRF1 in human atherosclerosis: colocalization and possible involvement in cell death of vascular endothelial cells. *Atherosclerosis* **161**, 281–291 (2002).
151. Fan, F. et al. ATF3 induction following DNA damage is regulated by distinct signaling pathways and over-expression of ATF3 protein suppresses cells growth. *Oncogene* **21**, 7488–7496 (2002).
152. Hoetzenecker, W. et al. ROS-induced ATF3 causes susceptibility to secondary infections during sepsis-associated immunosuppression. *Nat. Med.* **18**, 128–134 (2011).
153. Odiete, O., Hill, M. F. & Sawyer, D. B. Neuregulin in cardiovascular development and disease. *Circ. Res.* **111**, 1376–1385 (2012).
154. De Keulenaer, G. W. et al. Mechanisms of the multitasking endothelial protein NRG-1 as a compensatory factor during chronic heart failure. *Circ. Heart Fail.* **12**, e006288 (2019).
155. Wang, Z. N. et al. Cell-type-specific gene regulatory networks underlying murine neonatal heart regeneration at single-cell resolution (vol 33, 108472-1.e1, 2020). *Cell Rep.* **35**, 109211 (2021).
156. Zhuang, L., Lu, L., Zhang, R., Chen, K. & Yan, X. Comprehensive integration of single-cell transcriptional profiling reveals the heterogeneities of non-cardiomyocytes in healthy and ischemic hearts. *Front. Cardiovasc. Med.* **7**, 615161 (2020).
157. Li, Z. et al. Single-cell transcriptome analyses reveal novel targets modulating cardiac neovascularization by resident endothelial cells following myocardial infarction. *Eur. Heart J.* **40**, 2507–2520 (2019).
158. Peisker, F. et al. Mapping the cardiac vascular niche in heart failure. *Nat. Commun.* **13**, 3027 (2022).
159. Kalucka, J. et al. Single-cell transcriptome atlas of murine endothelial cells. *Cell* **180**, 764–779.e20 (2020).
160. Rauch, A. et al. On the versatility of von Willebrand factor. *Mediterr. J. Hematol. Infect. Dis.* **5**, e2013046 (2013).
161. Randi, A. M., Smith, K. E. & Castaman, G. von Willebrand factor regulation of blood vessel formation. *Blood* **132**, 132–140 (2018).
162. Bedenbender, K. & Schmeck, B. T. Endothelial ribonuclease 1 in cardiovascular and systemic inflammation. *Front. Cell Dev. Biol.* **8**, 576491 (2020).
163. Amsellem, V. et al. ICAM-2 regulates vascular permeability and N-cadherin localization through ezrin-radixin-moesin (ERM) proteins and Rac-1 signalling. *Cell Commun. Signal.* **12**, 12 (2014).
164. Machon, O., Masek, J., Machonova, O., Krauss, S. & Kozmik, Z. Meis2 is essential for cranial and cardiac neural crest development. *BMC Dev. Biol.* **15**, 40 (2015).
165. Vanlandewijck, M. et al. A molecular atlas of cell types and zonation in the brain vasculature. *Nature* **554**, 475–480 (2018).
166. Hu, Z. et al. Single-cell transcriptomic atlas of different human cardiac arteries identifies cell types associated with vascular physiology. *Arterioscler. Thromb. Vasc. Biol.* **41**, 1408–1427 (2021).
167. Wirka, R. C. et al. Atheroprotective roles of smooth muscle cell phenotypic modulation and the TCF21 disease gene as revealed by single-cell analysis. *Nat. Med.* **25**, 1280–1289 (2019).
168. Chen, W. et al. Single-cell transcriptomic landscape of cardiac neural crest cell derivatives during development. *EMBO Rep.* **22**, e52389 (2021).
169. La Manno, G. et al. RNA velocity of single cells. *Nature* **560**, 494–498 (2018).
170. Bergen, V., Lange, M., Peidli, S., Wolf, F. A. & Theis, F. J. Generalizing RNA velocity to transient cell states through dynamical modeling. *Nat. Biotechnol.* **38**, 1408–1414 (2020).
171. Swirski, F. K. & Nahrendorf, M. Cardioimmunology: the immune system in cardiac homeostasis and disease. *Nat. Rev. Immunol.* **18**, 733–744 (2018).
172. Chakarov, S. et al. Two distinct interstitial macrophage populations coexist across tissues in specific subtissular niches. *Science* https://doi.org/10.1126/science.aau0964 (2019).
173. Hulsmans, M. et al. Macrophages facilitate electrical conduction in the heart. *Cell* **169**, 510–522.e20 (2017).
174. Lavine, K. J. et al. Distinct macrophage lineages contribute to disparate patterns of cardiac recovery and remodeling in the neonatal and adult heart. *Proc. Natl Acad. Sci. USA* **111**, 16029–16034 (2014).
175. Lavine, K. J. et al. The macrophage in cardiac homeostasis and disease: JACC macrophage in CVD series (Part 4). *J. Am. Coll. Cardiol.* **72**, 2213–2230 (2018).
176. Bajpai, G. et al. The human heart contains distinct macrophage subsets with divergent origins and functions. *Nat. Med.* **24**, 1234–1245 (2018).
177. Bajpai, G. et al. Tissue resident CCR2− and CCR2+ cardiac macrophages differentially orchestrate monocyte recruitment and fate specification following myocardial injury. *Circ. Res.* **124**, 263–278 (2019).
178. Dick, S. A. et al. Self-renewing resident cardiac macrophages limit adverse remodeling following myocardial infarction. *Nat. Immunol.* **20**, 29–39 (2019).
179. Zaman, R. et al. Selective loss of resident macrophage-derived insulin-like growth factor-1 abolishes adaptive cardiac growth to stress. *Immunity* **54**, 2057–2071.e6 (2021).
180. Bizou, M. et al. Cardiac macrophage subsets differentially regulate lymphatic network remodeling during pressure overload. *Sci. Rep.* **11**, 16801 (2021).
181. Cahill, T. J. et al. Tissue-resident macrophages regulate lymphatic vessel growth and patterning in the developing heart. *Development* https://doi.org/10.1242/dev.194563 (2021).
182. Badorff, C., Noutsias, M., Kuhl, U. & Schultheiss, H. P. Cell-mediated cytotoxicity in hearts with dilated cardiomyopathy: correlation with interstitial fibrosis and foci of activated T lymphocytes. *J. Am. Coll. Cardiol.* **29**, 429–434 (1997).
183. Barin, J. G. & Cihakova, D. Control of inflammatory heart disease by CD4+ T cells. *Ann. N. Y. Acad. Sci.* **1285**, 80–96 (2013).
184. Vdovenko, D. & Eriksson, U. Regulatory role of CD4(+) T cells in myocarditis. *J. Immunol. Res.* **2018**, 4396351 (2018).
185. Ong, S. et al. Natural killer cells limit cardiac inflammation and fibrosis by halting eosinophil infiltration. *Am. J. Pathol.* **185**, 847–861 (2015).
186. Nagy, C. et al. Single-nucleus transcriptomics of the prefrontal cortex in major depressive disorder implicates oligodendrocyte precursor cells and excitatory neurons. *Nat. Neurosci.* **23**, 771–781 (2020).
187. Liang, D. et al. Cellular and molecular landscape of mammalian sinoatrial node revealed by single-cell RNA sequencing. *Nat. Commun.* **12**, 287 (2021).
188. Goodyer, W. R. et al. Transcriptomic profiling of the developing cardiac conduction system at single-cell resolution. *Circ. Res.* **125**, 379–397 (2019).
189. Raredon, M. S. B. et al. Comprehensive visualization of cell-cell interactions in single-cell and spatial transcriptomics with NICHES. *bioRxiv* https://doi.org/10.1101/2022.01.23.477401 (2022).
190. Xiong, H. et al. Single-cell transcriptomics reveals chemotaxis-mediated intraorgan crosstalk during cardiogenesis. *Circ. Res.* **125**, 398–410 (2019).
191. Dann, E., Henderson, N. C., Teichmann, S. A., Morgan, M. D. & Marioni, J. C. Differential abundance testing on single-cell data using k-nearest neighbor graphs. *Nat. Biotechnol.* **40**, 245–253 (2022).
192. Dellefave, L. & McNally, E. M. The genetics of dilated cardiomyopathy. *Curr. Opin. Cardiol.* **25**, 198–204 (2010).
193. Rajewsky, N. et al. Publisher correction: LifeTime and improving European healthcare through cell-based interceptive medicine. *Nature* **592**, E8 (2021).
194. Churko, J. M. et al. Defining human cardiac transcription factor hierarchies using integrated single-cell heterogeneity analysis. *Nat. Commun.* **9**, 4906 (2018).
195. Ruan, H. et al. Single-cell reconstruction of differentiation trajectory reveals a critical role of ETS1 in human cardiac lineage commitment. *BMC Biol.* **17**, 89 (2019).
196. Paik, D. T. et al. Large-scale single-cell RNA-seq reveals molecular signatures of heterogeneous populations of human induced pluripotent stem cell-derived endothelial cells. *Circ. Res.* **123**, 443–450 (2018).
197. Friedman, C. E. et al. Single-cell transcriptomic analysis of cardiac differentiation from human PSCs reveals HOPX-dependent cardiomyocyte maturation. *Cell Stem Cell* **23**, 586–598.e8 (2018).
198. Wang, H., Yang, Y., Qian, Y., Liu, J. & Qian, L. Delineating chromatin accessibility re-patterning at single cell level during early stage of direct cardiac reprogramming. *J. Mol. Cell Cardiol.* **162**, 62–71 (2022).
199. Sim, C. B. et al. Sex-specific control of human heart maturation by the progesterone receptor. *Circulation* **143**, 1614–1628 (2021).
200. Ni, X. et al. Single-cell analysis reveals the purification and maturation effects of glucose starvation in hiPSC-CMs. *Biochem. Biophys. Res. Commun.* **534**, 367–373 (2021).
201. Giacomelli, E. et al. Human-iPSC-derived cardiac stromal cells enhance maturation in 3D cardiac microtissues and reveal non-cardiomyocyte contributions to heart disease. *Cell Stem Cell* **26**, 862–879.e11 (2020).
202. Zhou, Y. et al. Single-cell transcriptomic analyses of cell fate transitions during human cardiac reprogramming. *Cell Stem Cell* **25**, 149–164.e9 (2019).
203. Liu, Z. et al. Single-cell transcriptomics reconstructs fate conversion from fibroblast to cardiomyocyte. *Nature* **551**, 100–104 (2017).
204. Krane, M. et al. Sequential defects in cardiac lineage commitment and maturation cause hypoplastic left heart syndrome. *Circulation* **144**, 1409–1428 (2021).
205. Lam, Y. Y. et al. Single-cell transcriptomics of engineered cardiac tissues from patient-specific induced pluripotent stem cell-derived cardiomyocytes reveals abnormal developmental trajectory and intrinsic contractile defects in hypoplastic right heart syndrome. *J. Am. Heart Assoc.* **9**, e016528 (2020).
206. Mehrabi, M. et al. A study of gene expression, structure, and contractility of iPSC-derived cardiac myocytes from a family with heart disease due to LMNA mutation. *Ann. Biomed. Eng.* **49**, 3524–3539 (2021).
207. Kathiriya, I. S. et al. Modeling human TBX5 haploinsufficiency predicts regulatory networks for congenital heart disease. *Dev. Cell* **56**, 292–309.e9 (2021).

Acknowledgements

S.A.T. is supported by a Wellcome Sanger Institute grant (WT206194) and the Wellcome Science Strategic Support for a Pilot for the Human Cell Atlas (WT211276/Z/18/Z). N.H. is the recipient of an ERC Advanced Grant under the European Union Horizon 2020 Research and Innovation Program (AdG788970) and the Federal Ministry of Education and Research of Germany in the framework of CaRNAtion (031L0075A). M.D.S. received funding from the British Heart Foundation (CH/08/002/292257, RE/13/4/30184, RG/15/1/31165) and the European Research Council (233158). R.P.H. is supported by a National Health and Medical Research Council of Australia Investigator Grant (2021/GNT20087443) and Ideas

Grant (2020/GNT2000615). M.N. received funding from the British Heart Foundation (PG/16/47/32156). S.A.T., N.H. and M.N. have received funding from a BHF/DZHK grant (SP/19/1/34461) and from the Chan Zuckerberg Initiative (2021-237882 and 2019-202666). The authors thank E. Adami (Max-Delbrück-Center for Molecular Medicine in the Helmholtz Association, Berlin, Germany) for her help with Table 1.

Author contributions

A.M.A.M., V.J., H.M., K.K., J.C., M.D.S. R.P.H. and M.N. researched data for the article. and wrote the manuscript. A.M.A.M., V.J., H.M., K.K., S.A.T., N.H., M.D.S., R.P.H. and M.N. contributed to the discussion of content. All authors reviewed and edited the manuscript before submission.

Competing interests

S.A.T. has consulted for or has been a member of scientific advisory boards at Biogen, ForeSite Labs, Genentech, GlaxoSmithKline, Qiagen and Roche, and is an equity holder of Transition Bio. All other authors declare no competing interests.

Additional information

Correspondence should be addressed to Antonio M. A. Miranda or Michela Noseda.

Peer review information *Nature Reviews Cardiology* thanks David Paik and the other, anonymous, reviewer(s) for their contribution to the peer review of this work.